ISTANBUL TECHNICAL UNIVERSITY★GRADUATE SCHOOL OF SCIENCE ENGINEERING AND TECHNOLOGY

EFFECTS OF SPATIAL DISTRIBUTION OF FULLERENES ON THE MECHANICAL BEHAVIOR OF GRAPHENE FULLERENE COMPOSITES

M.Sc.THESIS

Uğur ŞİMŞEK
(503131510)

Department of Mechanical Engineering

Solid Mechanics Programme

Thesis Advisor: Assist.Prof.Dr.Mesut KIRCA

SEPTEMBER 2016

İSTANBUL TEKNİK ÜNİVERSİTESİ★FEN BİLİMLERİ ENSTİTÜSÜ

FARKLI FULLEREN DAĞILIMLARININ GRAFEN-FULLEREN KOMPOZİT MALZEMESİNİN MEKANİK DAVRANIŞINA ETKİSİNİN İNCELENMESİ

YÜKSEK LİSANS TEZİ

Uğur ŞİMŞEK
(503131510)

Makina Mühendisliği Anabilim Dalı

Katı Cisimlerin Mekaniği Yüksek Lisans Programı

Tez Danışmanı: Yard.Doç. Dr. Mesut KIRCA

EYLÜL 2016

Uğur ŞİMŞEK, a M.Sc. student of ITU Graduate of Science Engineering and Technology student ID 503131510, successfully defended the thesis entitled "EFFECTS OF SPATIAL DISTRIBUTION OF FULLERENES ON THE MECHANICAL BEHAVIOR OF GRAPHENE FULLERENE COMPOSITES", which he prepared after fulfilling the requirements specified in the associated legislations, before the jury whose signatures are below.

Thesis Advisor: **Assist. Prof. Dr. Mesut KIRCA** ....
Istanbul Technical University

Jury Members: **Assist. Prof. Dr. Atakan ALTINKAYNAK** ....
Istanbul Technical University

Assist. Prof. Emrecan SÖYLEMEZ ....
Marmara University

Date of Submission: 15 September 2016
Date of Defence: 29 September 2016

To my family,

FOREWORD

This thesis would not have been possible without a great deal of support.

I would especially like to thank Assist. Prof. Dr. Mesut KIRCA for being supervisor of this study, his suggestions, scientific and moral supports.

Finally, infinite thanks to my family for their understanding and encouragement through my life.

September 2016 Uğur ŞİMŞEK

Mechanical Engineer

TABLE OF CONTENTS

Page
FOREWORD .... **ix**
TABLE OF CONTENTS .... **xi**
ABBREVIATIONS .... **xiii**
LIST OF TABLES .... **xv**
LIST OF FIGURES .... **xviiivii**
SUMMARY .... **xix**
ÖZET .... **xxi**
1. INTRODUCTION **1**
2. NANOMATERIALS **5**
  2.1 Historical Background 5
  2.2 Introduction to Nano Science 7
  2.3 Formation of Nanomaterials 8
  2.4 Applications of Nanomaterials 10
3. CARBON NANOSTRUCTURES **13**
  3.1 Fullerene Structure and Properties 14
    3.1.1 Structure of fullerene 15
    3.1.2 Fullerene production 16
      3.1.2.1 Arc heating of graphite 16
      3.1.2.2 Fullerenes by pyrolysis 17
      3.1.2.3 Fullerene synthesis in combustion 18
      3.1.2.4 Fullerenes by concentrated solar flux 18
    3.1.3 Physical properties of fullerene 19
  3.2 Graphene Structure and Properties 19
    3.2.1 Graphene Production 22
      3.2.1.1 Exfoliation and cleavage 22
      3.2.1.2 Thermal chemical vapor deposition techniques 23
      3.2.1.3 Thermal deposition of SiC 24
    3.2.2 Physical properties of graphene 26
4. OVERVIEW OF MOLECULAR DYNAMIC SIMULATIONS **29**
  4.1 Introduction to Molecular Dynamics 29
  4.2 Historical Background 32
  4.3 Molecular Dynamics Foundation 32
    4.3.1 Basic theory 34
    4.3.2 MD limitations 36
5. MODEL GENERATION **37**
  5.1 Lamps Script Generation and MD Model Creation 37
    5.1.1 Initialization phase 38
    5.1.2 Atom definition phase 41
    5.1.3 Force field definition phase 44
      5.1.3.1 Lennard-Jones potential 44
      5.1.3.2 AIREBO potential 45
    5.1.4 Minimization phase 45

5.1.5 Equilibration phase 46
5.1.6 Deformation phase 50
5.2 Overall Simulation Options and Scope of MD Simulations 50
6. RESULTS AND DISCUSSIONS 53
6.1 Ordered and Randomly Distributed Fullerenes Between Graphene Layers Models Compressive Behavior Comparison Under Constant Strain Rate and Temperature 55
6.2 Ordered and Randomly Distributed Fullerenes Between Graphene Layers Models Compressive Behavior Comparison Under Constant Strain Rate and Various Temperatures 60
6.3 Ordered and Randomly Distributed Fullerenes Between Graphene Layers Models Compressive Behaviour Comparison Under Various Strain Rate and Constant Temperatures 63
7. CONCLUSION AND RECOMMENDATIONS 677
REFERENCES 69
APPENDICES 71
APPENDIX A 72
CURRICULUM VITAE 77

ABBREVIATIONS

CNTs **:** Carbon Nanotubes
MD **:** Molecular Dynamics
CVD **:** Chemical Vapour Decomposition
FEM **:** Finite Element Method
HOPG **:** Highly Oriented Pyrolytic Graphite
AFM **:** Atomic Force Microscope
TEM **:** Transmission Electron Microscope
GO **:** Graphite Oxide
CMOS **:** Complementary Metal Oxide Semiconductor
CFD **:** Heat Affected Zone
NMR **:** Nuclear Magnetic Resonance

LIST OF TABLES

Page

Table 2.1: Typical dimensions of nanomaterials.. **7**

LIST OF FIGURES

Page

Figure 2.1: The Lycurgus Cub [11]...... **6**
Figure 2.2: Scheme of Top-down and bottom up approaches to the synthesis of metal nanoparticles (MNP) [13]. **9**
Figure 3.1: The face-centred cubic cell of fullerene C60 [11]...... **15**
Figure 3.2: Schematic illustration of the arc heating apparatus for generating fullerene [20]...... **17**
Figure 3.3: Schematic illustration of the combustion synthesis of fullerenes [21]... **18**
Figure 3.4: Graphene based carbon materials. Graphene, Graphite, CNTs and Fullerene [22]...... **20**
Figure 3.5: Graphene is mother of all graphitic forms [23]...... **21**
Figure 3.6: Schematic of a common setup for chemical vapor deposition of graphene [24]...... **24**
Figure 3.7: Various thermal decomposition of SiC methods for generating graphene. **25**
Figure 5.1: Periodic boundary conditions. The atom at A, when moving to the position A^I outside the central simulation box, will instead be translated at B. All the atoms and periodic images of atoms interacting with atom labeled C are shown inside the big dotted circle [25]...... **39**
Figure 5.2: Link-cell algorithm in two dimensions. To compute the interactions with the atom labeled A, all the atoms inside the same sub-cell as A are considered, as well as all the atoms in the adjacent sub-cells within the cutoff radius [25]...... **41**
Figure 5.3: Randomly fullerene distributed atomistic model of nano-sandwiched foam...... **42**
Figure 5.4: Cross-sections (top views) of randomly and evenly generated fullerene-graphene composite specimens: (a) Hexagonal arrangement (b) Square arrangement (c) Rotated-Hexagonal arrangement (d) Random arrangement...... **43**
Figure 5.5: Lennard-Jones potential...... **45**
Figure 6.1: Potential energy profile of the nano-sandwiched models with time. The energy is normalized per atom...... **54**
Figure 6.2: Temperature stabilization during the thermalization period for various temperature levels. **54**
Figure 6.3: Comparison stress-strain curves for the nano-sandwiched structures with different types of fullerene arrangement under 300K room temperature and 0.002 1/ps strain rate...... **56**
Figure 6.4: Snapshots from compressive testing of Fullerene-graphene foam with hexagonal fullerene arrangement under 300K room temperature and 0.002 1/ps strain rate...... **57**
Figure 6.5: Snapshots from compressive testing of Fullerene-graphene foam with rotated-hexagonal fullerene arrangement under 300K room temperature and 0.002 1/ps strain rate...... **58**

Figure 6.6: Snapshots from compressive testing of Fullerene-graphene foam with randomly fullerene arrangement under 300K room temperature and 0.002 1/ps strain rate. **60**

Figure 6.7: Hexagonal fullerene arrangement results under various temperature at 0.002 1/ps strain rate. **61**

Figure 6.8: Square fullerene arrangement stress-strain curve under various temperatures at 0.002 1/ps strain rate. **62**

Figure 6.9: Rotated-hexagonal fullerene arrangement results under various temperature at 0.002 1/ps strain rate. **62**

Figure 6.10: Randomly fullerene arrangement results under various temperature at 0.002 1/ps strain rate. **63**

Figure 6.11: Hexagonal fullerene arrangement stress-strain curve under various strain rate 300 K. **64**

Figure 6.12: Square fullerene arrangement stress-strain curve under various strain rate 300 K. **64**

Figure 6.13: Rotated-Hexagonal fullerene arrangement stress-strain curve under various strain rate at 300 K. **65**

Figure 6.14: Randomly fullerene arrangement stress-strain curve under various strain rate at 300 K. **65**

EFFECTS OF SPATIAL DISTRIBUTION OF FULLERENE ON THE MECHANICAL BEHAVIOR OF GRAPHENE FULLERE COMPOSITES

SUMMARY

Carbon based nanostructures such as carbon nanotubes (CNTs), graphene and fullerenes have attracted great attention due to their remarkable thermal, mechanical and electrical properties. In the last years, hybrid carbon nanomaterials, which enable to construct higher scale, tailorable materials consisting of coupled nanostructures such as graphene-CNT, fullerene-CNT and graphene-fullerene, are in the focus of researchers. In this respect, this study examines the mechanical characteristics of a hybrid nanostructured material that consists of fullerenes covalently sandwiched between parallel graphene sheets. After checking stability of the covalent junctions and thermodynamic feasibility of the overall nanostructure by monitoring the free energy profiles over a sufficiently long period through molecular dynamics simulations (MD),as the main objective of this study, the effects of layerwise spatial distribution of fullerenes on the compressive mechanical properties are investigated. For this purpose, atomistic models for the proposed fullerene-graphene composite structures are generated by the use of C_{180} fullerene with different spatial arrangements between graphene sheets. Random and ordered type fullerene dispersions are considered as two main fullerene distribution schemes employed in the atomistic modelling process. Comparisons are performed between fullerene-graphene composite structures with randomly and evenly distributed fullerenes in terms of elastic mechanical properties and energy absorbing characteristics. In this regard, compressive loading tests at different strain rates and various temperatures are performed via MD simulations to capture the mechanical response of sandwiched fullerene-graphene structures with different fullerene arrangements.

In the MD simulations, the four nanostructures were assumed to be different spatial fullerene arrangement between graphene layers and results were compared. It was found that spatial distribution of fullerenes has remarkable influence on both compressive stress level and stress-strain characteristic of the novel fullerene – graphene foams. Mechanical response of the hexagonal and square fullerene arrangement models are in good agreement with both each other and conventional foam materials while rotated hexagonal and randomly fullerene distributed models are exhibited totally unique mechanical behaviours due to their special structures. In addition to investigation of spatial fullerene distribution effects on mechanical properties of the fullerene-graphene specimens, temperature and strain rate sensitivity of nano foams are studied in this thesis. As a consequence of certain MD simulation results, applied temperatures have no major impact on stress-strain curve tendency; however, young modulus of the materials tend to decrease with higher employed temperature level. In parallel that mechanical tests of fullerene-graphene foams under uniaxial compression show that the form of the stress-strain diagram does not depend on the applied strain rates. However, higher strain rates in general lead to higher stresses under compression at the beginning of the plateau regime and densification phase.

FARKLI FULLEREN DAĞILIMLARININ GRAFEN-FULLEREN KOMPOZİT MALZEMESİNİN MEKANİK DAVRANIŞINA ETKİSİNİN İNCELENMESİ

ÖZET

Son yıllarda ortaya konulan ciddi deneysel ve teorik araştırmalara paralel olarak, nanoteknoloji içerisinde önemli bir yer sahibi olan ‘nanomalzemeler’ önemli ve ilgi çeken bir bilim alanı olmuştur. Bir çok çalışma göstermiştir ki; yakın gelecekte, daha kompleks mühendislik yapılarının meydana getirilmesinde nanomalzemelerin üstün fiziksel ve kimyasal özelliklerinden ciddi oranda yararlanılacaktır. Örneğin, konvansiyonel malzemelerden daha iyi performansa sahip ultra hafif malzemelerin dizaynı yakın gelecekte mümkün olacaktır. Bu açıdan değerlendirildiğinde, karbon temelli malzemeler, grafen, karbon nanotüpler (CNTs) ve fulleren her disiplinden bir çok araştırmacının dikkatini çekmektedir.

Karbon yapılı malzemelerin doğasını anlamak için karbonun elektronik yapısının detaylı olarak incelenmesi ve bilinmesi gerekir.Karbon 6 elektronlu ($1s^2$, $2s^2$, $2p^2$) yapısıyla diğer bir çok element ile kolay bağ kuran bir yapıya sahiptir. Bunla beraber karbon kendi içerisinde de bağ kurabilir ve bu sebeple doğada allotroplarıyla bilinen bir elementtir. Elmas ve grafit karbon allotrobu olarak uzun çağlardır bilinmektedir. Ancak tamamen yeni karbon formları olan fulleren, grafen ve karbon nanotupler son 30 yılda bulunan yeni karbon formlarıdır.

Fulleren ilk olarak ‘buckminsterfullerene’ ismiyle Kroto tarafından 1985 yılında rapor edilmiştir.C60 molekülü en yaygın bilinen fulleren yapısıdır ve 12 tane beşgen, 20 tane altıgen yüzeyin simetrik olarak dizilmesiyle elde edilen küresel bir moleküldür. Bu yapısıyla fulleren, Euler teoremine uyum sağlamaktadır. Fulleren sp^2 bağ yapısıyla çok güçlü bir moleküler yapıya sahiptir ve çok büyük basınç yüklerine karşı dayanım gösterebilir. Fullerenler 3000 atmosfer basınca maruz kaldıktan sonra üzerindeki yük kaldırıldığında, ilk hallerine dönebilecek kadar dayanımı yüksek malzemelerdir. Bu açıklamaya paralel olarak teorik hesaplar göstermektedir ki bir C60 molekülünün elastiklik modülü yaklaşık olarak 668 GPa mertebesindedir.

Fullerenlerden farklı olarak, grafen, iki boyutlu kristal bir yapıya sahiptir. Grafitten çeşitli üretim teknikleriyle elde edilen, tek atom kalınlığında karbon atomlarının altıgen formda yerleşmesiyle elde edilmektedir. İlk kez 2004 yılında üretimi gerçekleştirilmiştir ve o tarihten itibaren bilim ve endüstri dünyasından bir çok araştırmacının ilgisini çekmiştir. Yapılan çalışmalar sonucunda grafenin elastiklik modülünün 500 GPa mertebesinde olduğu bilinmektedir. Grafen %15 gerinim altında dahi serbest bırakıldığında ilk haline dönebilmektedir.

Bu çalışmada, grafen katmanlarının arasına fulleren yapıları yerleştirilerek tamimiyle yeni bir malzeme modeli önerilmiş ve mekanik özellikleri incelenmiştir. Test modellerinde fullerenler grafen katmanları arasına rastgele ve düzenli olarak yerleştirilerek,,grafen katmanları üzerindeki dağılımlarının, malzemenin mekanik özelliklerine ve enerji depolama kabiliyetine etkisi incelenmiştir. Bu amaçla fullerenlerin altıgen, kare, döndürülmüş altıgen ve rastgele dağıltılmasıyla 4 farklı test

modeli oluşturulmuştur. Her test modeli on bir grafen katmanından oluşmaktatır. Bu çalışmada C180 tipi fulleren yapıları kullanılmıştır. Bu varsayımlar kullanılarak, mekanik davranışlarının incelenmesi maksadıyla her dört farklı fulleren dağılımına sahip test numunelerinin moleküler dinamik (MD) yöntemiyle basma yükü altındaki davranışı incelenmiştir.

Temel olarak MD kompleks malzeme sistemlerinin mekanik davranışlarının bilgisayar ortamında atomik seviyede incelenmesine olarak sağlayan bir tekniktir. Geçmişte bilimin ilerlemesi tamimiyle deneysel ve teorik çalışmalara dayanmaktaydı. Ancak atomik boyutta istenilen deneylerin yapılabilmesi çoğu zaman mümkün olmamakla beraber, gerçekleştirilebilen bir çok test ve deney ise çok yüksek teknolojiye ihtiyaç duyduğundan oldukça pahalıdır. Öte yandan teorik çalışmalar ise analitik ve nümerik olarak bir çok varsayıma dayandığı için ancak limitli sayıda özel durumlar için kullanılabilir durumdadır. İşte tam bu noktada bilgisayar tabanlı MD metotları erişilebilir deneysel çalışmalarla teorik varsayımlar arasında bir köprü görevi görerek araştırmacılar için ciddi bir fırsat sunmaktadır.

MD metotları temelde fiziksel sistemin tanımlanmasına göre iki ayrı kategoriye ayrılmaktadır. Bunlardan ilki ‘klasik mekanik’ yaklaşımı olarak adlandırılmaktadır ve Newton fiziğine dayanmaktadır. İkinci yöntem ise ‘kuantum mekanik’ yöntemlerine dayanmaktadır ve bu yöntemde kimyasal bağların yapısı kuantum denklemeleri kullanılarak hesaplanmaktadır. İlk olarak 1980’li yılların başlarında kullanılmaya başlanılan kuantum tabanlı MD metotları, klasik MD yöntemlerine göre çok daha doğru sonuçlar sağlamaktadır. Ancak kuantum tabanlı MD simülasyonları çok daha fazla bilgisayar kapasitesine ihtiyaç duymaktadır. Bu sebeple ancak daha küçük modellerde, bir kaç nanosaniye mertebelerinde kullanımları mümkün olmaktadır. Öte yandan gerçek sonuçlardan belli hata miktarlarıyla sonuç veren klasik MD yöntemleri daha büyük yapıların daha uzun süreli olarak modellenmesine olanak vermesi açısından yaygın olarak tercih edilmektedir. Bu çalışmada da oluşturulan fulleren-grafen nano-kompozit malzemelerin mekanik davranışları, klasik MD yöntemi kullanılarak incelenmiştir.

Klasik MD programı olarak bu çalışmada ‘Large-scale Atomic/Molecular Massively Parallel Simulator (LAMMPS)’ kullanılmıştır. Ayrıca analiz sonuçlarının incelenmesi ‘Open Visualization Tool (OVITO)’ yardımıyla gerçekleştirilmiştir. Kullanılan moleküler dinamik programı atom modellemesine izin vermemektedir. Bu sebeple, nano-kompozit malzemeye ait atom koordinatları ‘MATLAB’ ortamında kod yardımıyla oluşturulup, daha sonra LAMMPS ortamına aktarılmıştır.

Atomlar moleküler dinamik simülasyon ortamına tanıtıldıktan sonra karbon atomları arasındaki bağ kuvvetlerini modellemek amacıyla ‘Adaptive intermolecular reactive bond order (AIREBO)’ potansiyeli kullanılmıştır. AIREBO potansiyeli karbon içeren yapılarda bağ kuvvetlerinin modellenmesinde en yaygın olarak kullanılan potansiyeldir. Ayrıca atomlar arasında fiziksel olmayan kuvvetlerin oluşmasını engellemek amacıyla karbon atomları arasında bağ oluşmuşumunda mesafe kontrolü kullanılmıştır. Bu çalışmada iki karbon arasında bağ kuvveti oluşması için tanımlanan maksimum mesafe 2 Angström olarak belirlenmiştir.

Karbon atomları arasındaki bağ kuvvetleri tanımlandıktan sonra, test modelleri simülasyon ortamında şartlandırılmıştır. Tüm test modellerinde basınç değeri sıfıra eşitlenmiştir. Böylelikle basma yükü uygulanmadan önce test modellerinde artık gerilme ortadan kaldırılmıştır.

Bu çalışmada fulleren atomlarının grafen katmanları arasına dağılımlarının, malzemenin mekanik özeliklerine etkisinin incelenmesine ek olarak, önerilen yeni malzemenin davranışının, sıcaklık ve gerinim hızına hassasiyeti de incelenmiştir. Bu amaçla basma yükü uygulanmadan önce test modelleri 300 K, 500 K ve 700 K sıcaklığında şartlandırılmış ve modellerin kararlı hale ulaştığından emin olunmuştur. Basma hızının malzemenin mekanik özeliklerine ve enerji sönümleme karakterine etkisini incelemek için ise modeller 0.002 ps^{-1}, 0.004 ps^{-1} ve 0.006 ps^{-1} gerinim hızlarında yüklenmiştir. Analizler tamamlandıktan sonra ise test modellerinin mekanik davranışlarını incelemek amacıyla gerilme-gerinim grafikleri oluşturulmuştur. Bu grafiklerle malzemelerin karakterlerinin belirlenmesine ek olarak, grafiklerin altında kalan alanın hesaplanmasıyla malzemelerin ne kadar enerji sönümlediği de hesaplanabilmiştir.

Bu çalışmanın sonucu olarak fullerenlerin, farklı uzaysal pozisyonlarda grafen katmanları arasında dağıtılması malzemenin basma gerilme seviyelerini değiştirmekle beraber malzemelere ait gerilme-gerinim grafiğinin karakteri üzerinde de ciddi bir etkisinin olduğu gözlemlenmiştir. Altıgen ve kare fulleren dağılımlarının mekanik ve enerji sönümleme karakteri konvansiyonel köpük malzemelerle benzerlik göstermesine rağmen, döndürülmüş altıgen ve rastgele fulleren dağılımlarının tamamen farklı davrandığı rapor edilmiştir.

Bu çalışmada sıcaklık ve gerinim hızına bağlı malzeme özelliklerindeki değişimler de incelenmiştir. Sonuç itibariyle; sıcaklığın malzeme davranışı üzerinde önemli bir etkisi olmadığı sonucuna varılmıştır. Ancak elastiklik modülünün sıcaklık artışıyla beraber düşme eğiliminde olduğu gözlemlenmiştir. Diğer bir parametre olan gerinim hızının ise, gerilme-gerinim grafiğinin karakterine etkisinin olmadığı sonucuyla beraber, yüksek gerinim hızlarının daha yüksek pik gerilme değerlerine sebep olduğu sonucuna varılmıştır.

1. INTRODUCTION

In the field of nanotechnology, the science of nanomaterials has become one of the most crucial and remarkable discipline in recent years as a consequence of extraordinary experimental and theoretical research effort. It is expected that in the near future increasing usage of nanomaterials will have much more significant impacts on the development of sophisticated engineering systems by utilizing their remarkable physical and chemical properties [1].For instance, it will be possible to design ultra-light structures by presenting much better performance in comparison with the conventional materials. Once considered from this point, carbon-based nanomaterials such as graphene, carbon nanotubes (CNTs) and fullerenes constitute a unique place among place among other nanomaterials and have attracted considerable attention by researchers all around the globe from different disciplines [2].

Due to its special chemical architecture, carbon is capable of forming many allotropes including diamond and graphite as the most known formations. On the other hand, over the past three decades, entirely new forms of carbon such as fullerene (Kroto, 1985) and carbon nanotubes (Lijima, 1991) have been synthesized [3]. As a consequence of those discoveries an accelerated research interest focused on C-based nanomaterials, which yielded another allotrope of carbon namely graphene that is one atom-thick layer of graphite crystal consisting of sp^2-hybridized planar sheets of carbon atoms [4].Thus, carbon community identified carbon allotropes regarding to its dimension; zero–dimensional fullerenes, one dimensional CNTs, two–dimensional graphene sheets and three dimensional diamond and graphite [5].

Graphene, the single layer of the graphite crystal, pure covalently bonded carbon in a honeycomb atom thick made of planar sheets of sp^2 – hybridized planar sheets of carbon atoms, represents a new two-dimensional (2D) material having the unique mechanical properties desired for a wide range of technological applications. As a consequences of many experimental and theoretical studies, graphene has been recognized by its extraordinary strength beyond any other material. With the thickness of only a few atomic layers, graphene breaking strength is around 42 N/m and its unique elastic modulus is 1.0 ± 0.1TPa [6]. In the view of recent research on mechanical specification of graphene, it is 100 times stronger than steel while it is flexible as rubber. Besides, graphene is tougher than its allotrope diamond and has the highest conductivity among any of the known that makes graphene 13 times more conductive than cooper [6]. We should mention that other novel forms of carbon, in fact they have been discovered before graphene, closely related to graphene. Graphene is the basic structural element of some carbon allotropes, including graphite, CNTs, and fullerenes. Fullerene is entirely composed of carbon in the form of spherical shapes called Bucky balls, whereas CNTs have tubular arrangements. For more than two decades, fullerene and CNTs-based materials enjoyed widespread applications in diverse fields of research such as electronics, batteries, super-capacitors, fuel cells, electrochemical sensors, and biosensor.

Over the past few decades, extensive research has been carried out to investigate and analyse the mechanical properties of nanostructures via experiments and simulations. In addition to experimental approaches, in particular, theoretical methods may be collected in three major separate group named (i) atomistic scale methods, (ii) continuum methods and (iii) atomistic-to-continuum coupling method. The molecular dynamics (MD) simulations have proven an effective approach defining the mechanical specifications of nano-structures as atomistic method [7]. Fundamentally, Molecular dynamics involves the calculation of the time-dependent movement of each atom in a molecule by solving Newton’s equations of motion. Essentially, MD predicts atomistic positions, velocities and forces of atoms in each time step and by this aspect, MD algorithms perfectly model nanostructures discrete nature. Moreover, atomistic simulations are advantageous in tracking the structural evaluation of mechanical behaviour of nano-structures compared to experiments of mechanical testing that are uneasy to design and perform in the fine scale. However, MD simulation for large and complex nano structures usually requires expensive computational facilities as well as intensive computation. Hence, these atomistic simulations are limited to very small length and time scales [8]. Thus, the notions of continuum methods and atomistic to continuum methods have attracted a great deal of attention of many researchers in order to overreach quite limited time length and atom numbers. Nevertheless, those methods has significant difficulties such as identification of different parameters in

MD-continuum interference and also they are computationally expensive for large scale and complex nanostructures [7, 9].

In the light of recent investigations summarized above, in this study, it is aimed to explore the mechanical behaviour of a novel hybridized carbon-based material, fullerenes penetrates graphene layers with different spatial fullerene arrangements, under uniaxial compressive loadings via very accurate MD simulations. Furthermore, this study has been initiated to examine energy absorption characteristic, understanding of the effects of the various strain rates on elastic/plastic strength, and thermalization temperature sensitivity of the Fullerene-graphene foam material.

2. NANOMATERIALS

The physical and chemical properties of nanomaterials can differ compared with macroscopic (bulk) materials built up from the same atoms or compounds. The production routes, characterization, and applications of materials sized on the nanometer scale also differ from the bulk. These differences between nanomaterials and the molecular and condensed-phase materials primarily are related to the spatial structures and shapes, phase changes, energetics, electronic structure, chemical reactivity, and catalytic properties of large, finite systems, and their assemblies. In this chapter,brief information about nanomaterials, their historical background, synthesis and applications of in modern world are collected and presented.

2.1 Historical Background

The term ‘nano’ comes from originally a Greek word, meaning ‘dwarf’. In scientific jargon, nano means 10^{-9}, thus, a nanometer is a billionth of a meter. That can be embodied in the light of some examples that nano is ten times the diameter of a hydrogen atom, or 1/80,000 of the diameter of a human hair. In fact, nanoparticle or an ultrafine particle is a small solid whose diameter lies in the range of 1 to 100 nanometers [10].

Although nanomaterials have attract enormous attention of the great number of researchers in the past a few decades, usage of nanomaterials is much older than today’s science, and dates back to ancient Egyptian, Chinese, and Roman times. It is certain that ancient and premodern age’s technologies could not explain and control material properties of nanomaterials, however, the nanomaterial production methods were quite enough to evoke admiration. In the ancient times metal nanoparticles were formed in molten glass, and used to make stained glass objects. The most famous sample of ancient glass is Lycurgus Cup, Fig. 2.1, illustrating myth of King Lycurgus housed up at the British Museum. The dispersed gold nanoparticles in the glass make it to appear green, when viewed in reflecting daylight. But, when the cup is illuminated from the inside it appears red by the transmitted light [11].

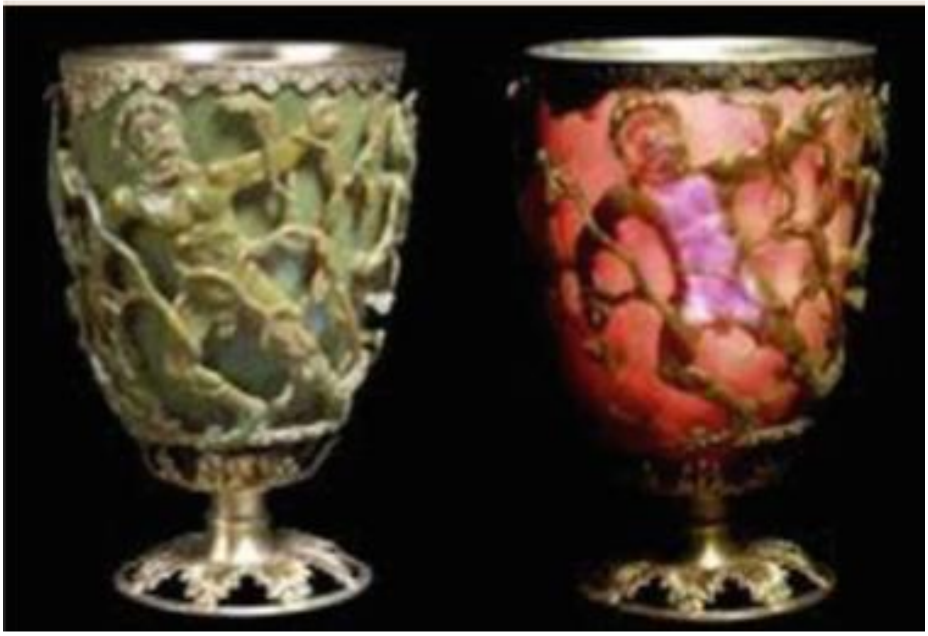

Figure 2.1: The Lycurgus Cub [11].

The first "scientific" study of metal nanoparticles was revealed by Michael Friday around 1850. As an eye-opening work, Faraday discovered that the red color of gold colloid was due to the minute size of the Au particles and that one could turn preparation blue by adding salt to the solution. After all accumulation of knowledge during the centuries, the idea of nanotechnology was published by Richard Feynman on December 1959 and the history of nanomaterials took an amazing turn in the mid of 20th century. Richard Feynman presented his famous lecture about the huge information storage capacity of materials if and when one goes to the atomic scale, to store ultimately one bit of information in every atom. In parallel, the discovery of semiconductor-based transistors by John Bardeen, William Shockly and Walter Brattain supported Feynman study and opened the road for miniaturization and integration enable to save space by making compact equipments. Today, semiconductor devices are finding several applications including from kitchen appliance to space-craft covering between them a large range of other applications. There have been huge achievements and obvious exponential growth in nanomaterial science, and commercialization of nanomaterials in the last 50 years. It is certain that great numbers of data and theoretical approaches will make the area of nanostructuring richer and a lot of new applications will come out in the close future.

2.2 Introduction to Nano Science

Nanoscience and nanotechnology deal with the synthesis, characterization, exploration, and exploitation of nanostructured materials which are small solids whose one dimension in the nanometre (1nm = 10^{-9} m) range at least. Nanostructures constitute a form between molecules and infinite bulk systems. Individual nanostructures include clusters, quantum dots, nanocrystals, nanowires, and nanotubes, while collections of nanostructures involve arrays, assemblies, and super lattices of the individual nanostructures. Table 2.1 lists typical dimensions of nanomaterials [12].

Table 2.1: Typical dimensions of nanomaterials

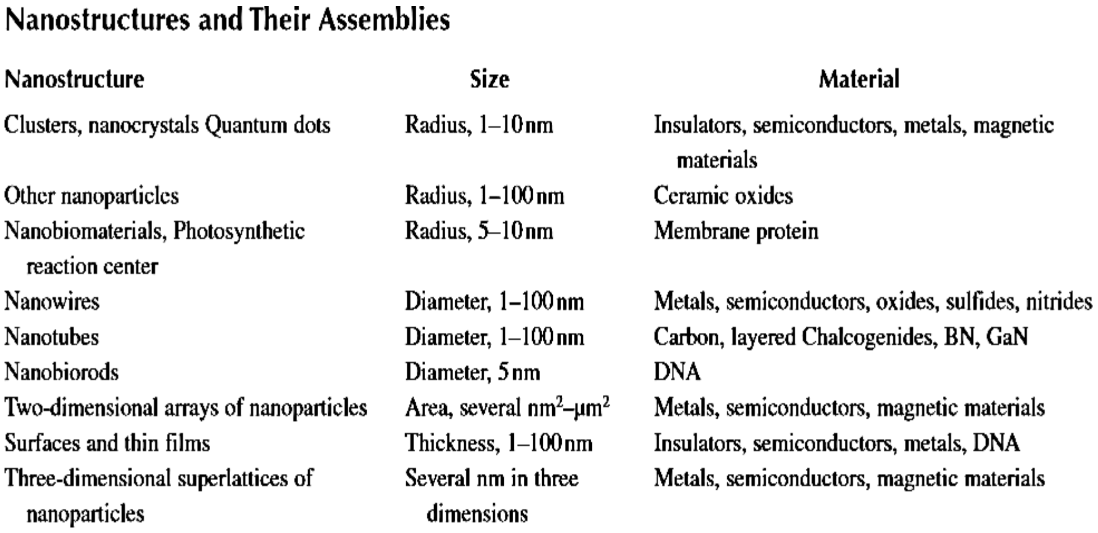

Nanostructures and Their Assemblies

Nanostructure	Size	Material
Clusters, nanocrystals Quantum dots	Radius, 1–10 nm	Insulators, semiconductors, metals, magnetic materials
Other nanoparticles	Radius, 1–100 nm	Ceramic oxides
Nanobiomaterials, Photosynthetic reaction center	Radius, 5–10 nm	Membrane protein
Nanowires	Diameter, 1–100 nm	Metals, semiconductors, oxides, sulfides, nitrides
Nanotubes	Diameter, 1–100 nm	Carbon, layered Chalcogenides, BN, GaN
Nanobiorods	Diameter, 5 nm	DNA
Two-dimensional arrays of nanoparticles	Area, several nm^2–μm^2	Metals, semiconductors, magnetic materials
Surfaces and thin films	Thickness, 1–100 nm	Insulators, semiconductors, metals, DNA
Three-dimensional superlattices of nanoparticles	Several nm in three dimensions	Metals, semiconductors, magnetic materials

The field of nanoscience and nanotechnology is interdisciplinary science which studied by physicists, chemists, material scientists, biologists, engineers, computer scientists, etc. Research in the field of nanoscience and nanotechnology have grown explosively in the last decade due to increasing availability of revolutionary instruments and approaches methods of synthesis of nanomaterials [12, 14]. Recently, the size-dependent electrical, optical, and magnetic properties of individual nanostructures of semiconductors, metals, and other materials can be better understood as a consequence of several innovative methods of synthesizing nanoparticles and nanotubes and their assemblies that allow the investigation of material properties with a resolution close to the atomic level.

The physical and chemical properties of nanostructures are distinctly different from corresponding single atom (molecule) and bulk matter bulk materials, which are same chemical composition, in many ways. These dissimilarities between nanomaterials and the molecular and condensed-phase materials pertain to the spatial structures and shapes, phase changes, energetics, electronic structure, chemical reactivity, and catalytic properties of large, finite systems, and their assemblies. Some of the important issues in nanoscience relate to size effects, shape phenomena, quantum confinement, and response to external electric and optical excitations of individual and coupled finite systems [12].At the other end of the size scale, materials start to be different from bulk below 100 nm size, because the effects of quantum confinement on electrical, thermal, and optical properties become significant at about this size.

New science established to describe the properties and behaviour of nanomaterials. In computations on nanomaterials, one deals with a spatial scaling from 1Å to 1µm and temporal scaling from 1fs to 1s, the limit of accuracy going beyond 1 kcal/mol. The present goals of the science and technology of nanomaterials are to master the synthesis of nanostructures (nano-building units) and their assemblies of desired properties; to explore and establish nano-device concepts; to generate new classes of high-performance nanomaterials, including biology-inspired systems; and to improve techniques for the investigation of nanostructures. Besides the established techniques of electron microscopy, crystallography, and spectroscopy, scanning probe microscopies have provided powerful tools for the study of nanostructures. Novel methods of fabricating patterned nanostructures as well as new device concept are being constantly discovered. Nanostructures also offer opportunities for meaningful computer simulation and modelling since their size is sufficiently small to permit considerable rigor in treatment. One potential applications of nanotechnology is the production of novel materials and devices in nanoelectronics, computer technology, medicine, and health care.

2.3 Formation of Nanomaterials

Synthesis and fabrication of nanomaterials are the most critical and important steps in the studies of nanoparticles. The ways in which nano materials are made vary widely, and discuss all of them are not aim of this study. However, it is important to understand some features of the processes used in the synthesis of nanomaterials, because the processing route often dominates the behavior of any given material. In a broad sense, formation of nano sized materials–nanoparticles, nanoporous or nanostructured macroscopic materials can be put into two categories: (i) Top-down method, and (ii) Bottom-up method.

In the Bottom-up approach that has been already known by chemists, one begins with a bulk material in the liquid, solid, or gas phase that is then employed to make a final nanomaterial structure by molecular level manipulations. On the other hands top-down method is opposite to bottom-up method. Top-down approach constructs the nano-structured topology starting from the macro-level materials instead of molecular level. It refers to a set of fabrication technologies which fabricate by removing methods, which can be mechanical, chemical, electrochemical, etc., depending on the material of the base substrate and requirement of the feature sizes, certain parts from a bulk material. Top-down and bottom-up methods are explained schematically at Figure 2.2.

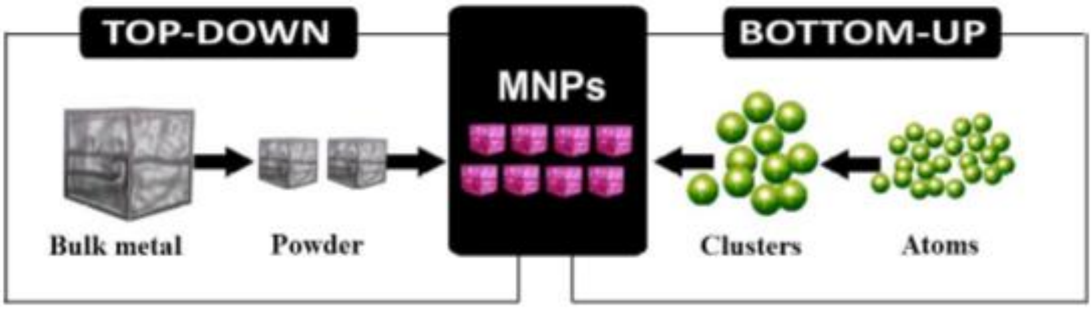

Figure 2.2: Scheme of Top-down and bottom up approaches to the synthesis of metal nanoparticles (MNP) [13].

Traditional fabrication operations for manufacturing include cutting, carving and molding are typical types of top-down method. By this approach, exceptional machinery and electronic devices have been able to be fabricated. However, due to limitations on the size of cutting, carving and molding capabilities, the size of these devices cannot be downsized beyond a certain limit. Nano-lithography, laser ablation, physical vapor deposition, electrochemical method (electroplating), milling and hydrothermal technique are the examples of techniques that are based on top-down approach. Bottom-up approach is being utilized by several nanoscale manufacturing techniques such as chemical vapor deposition (CVD), laser pyrolysis and molecular self-assembly. In this approach, atomic scale structural units, atoms, molecules or clusters, arrange themselves into more complex structural units similar to the growth of a crystal. It is evident that bottom-up approaches require control of processes at very fine scales, but this is not as difficult as it sounds, since chemical reactions essentially occur molecule by molecule (indeed, the nanomaterials made by nature are grown through bottom-up approaches) [14].

There are two approaches for synthesis of nano materials and the fabrication of nano structures and both approaches play very important role in modern industry and most likely in nano technology as well. There are advantages and disadvantages in both approaches. The major problem with top-down approach is the imperfection of surface structure and significant crystallographic damage to the processed patterns. These inadequacies cause to extra challenges in device design and fabrication process. Though the bottom up approach often referred in nanotechnology and also it has been in industrial use for over a century. Although the bottom up approach is nothing new, it plays an important role in the fabrication and processing of nano-structures. When structures fall into a nanometer scale, there is a little chance for top down approach. All the tools we have possessed are too big to deal with such tiny subjects. Bottom up approach also promises a better chance to obtain nano structures with less defects, more homogeneous chemical composition. On the contrary, top down approach most likely introduces internal stress, in addition to surface defects and contaminations.But this approach leads to the bulk production of nano material. Regardless of the defects produced by top down approach, they will continue to play an important role in the synthesis of nano structures.

2.4 Applications of Nanomaterials

Day by day, appearance of nanomaterials in scientific and industrial arena is increasing. Today, nanomaterials have already found applications in a very wide range of engineering fields including mechanical engineering and bioengineering. It is obvious to see nanomaterials regularly in our computers, wrinkle-free or stain-resistant textiles, self-cleaning windows, and suntan creams. In parallel to commercial application, a vast number of applications have been proposed in diverse fields in scientific area [11].

For the purposes of exposition how the nanocomposites including particles and fibers are used to reinforce or change of bulk material properties, it is the best way to provide some examples from the modern world applications. For instance, on glass bottles, to prevent sunlight damages novel UV-barrier coatings are used on the beverages. Tennis balls with much longer service life can be achieved by using butyl-rubber/nano-clay composites. As another example, nanoscale titanium dioxide is employed in cosmetics, sun-protective creams and self-cleaning windows. Along the same line, nanoscale silica is finding applications as a filler material in cosmetics and dental operations [13].

Some more examples can be given explaining the high interest concentrated on nanomaterials due to their unusual mechanical, electrical, optical and magnetic properties. For example, popularity of nanophase ceramics is mainly because of their higher ductility at extreme temperatures comparing to coarse-grained ceramics. Significant developments are occurring in the sintering of nanophase ceramic materials and in textiles and plastics containing dispersed nanoparticles. They are also good candidates for metal-metal bonding owing to their high valued cold welding properties in addition to their ductility. Remarkably high surface-to-volume ratio of nanoparticles leads to extraordinary improvements of chemical catalysis. The range of potential applications of nanoparticles in catalysis is very broad to be from fuel cell applications to catalytic converters and photocatalytic devices [13].

3. CARBON NANOSTRUCTURES

Materials science has supported the activities of humankind over the dozens of centuries. The researches on material science by using modern technology totally organize and revolute modern human way of live. By the view of accumulation of knowledge, chemical elements were collected in the periodic table because of researches extraordinary efforts and there is no hesitate that one of the most attractive element in this table is certainly carbon [15]. Historically, the term carbon, was named by Antoine L. de Lavoisier in 1789 firstly, originates from Latin ‘carbo’ for charcoal. Indeed, for the centuries carbon based materials have used by humankind in wide range of applications in parallel with progress of civilization [16].

In order to understand the nature of carbon based materials, it is necessary to research the electronic structure of carbon atom extensively. Carbon contains six electrons ($1s^2$, $2s^2$, $2p^2$) and the carbon element introduce unique bonding possibilities. Carbon may easily bond to great number of other elements and the electronic configuration of carbon-based structure identifies specification of the material. Besides, carbon can bond itself because of its unique nature, thus, is known well its allotropes [16]. The several hybridization states of carbon (sp, sp^2, and sp^3) can lead to numerous carbon allotropes, such as diamond (sp^3), graphite (sp^2), fullerene (sp^2), carbon nanotubes (sp^2), and graphene (sp^2). Although graphite and diamond were known to be different configuration of the same element over the centuries, fullerene, carbon nanotubes (CNTs) and graphene were discovered in the last two decades of 20th Century.

This chapter is particularly concern with the supreme properties and enormous potential applications of carbon-based materials, respectively, third major carbon form fullerenes, and graphene. These carbon-based materials have attracted huge amount of funding for scientific projects as well as driven extensive research efforts associated with exceptional mechanical, optical, and electrical properties.

3.1 Fullerene Structure and Properties

Carbon was only known to in two exist forms diamond and graphite until entirely new form named ‘buckminsterfullerene’ was discovered by Kroto in 1985 [17]. Great number of invention have been carried out in order to present huge potential of this new carbon allotrope. Hence a new field in materials science was established which attracted enormous attention of different disciplines such as medicine, physics, chemistry, mathematics, and engineering. The discovery of buckminsterfullerene or well-known name ‘C_{60}’ was awarded the Nobel Prize in Chemistry [11].

Although the discovery of C_{60} as a spherical icosahedral (Ih) carbon molecule was reported in 1985, other researchers thought about it before. Schultz in 1965 showed the possibility of having different kinds of carbon-hydrogenated cages; among them, the ‘Ih’ truncated icosahedron of C_{60}. In 1970, Osawa published a paper in the Japanese journal Kagaku proposed that C_{60}, the spherical Ih – symmetric football structure, is a possible structure [18]. Orville L.Chapman started the first experiments towards chemical synthesis of C_{60} at the beginning of the 1980s, before the discovery of C_{60}.

Thirty years have passed since the soccerball molecule first occurred in the minds of theorists, which is now generally recognized as being representative of a new class of carbons known as fullerenes. Fullerenes have a closed hollow network of small rings, each consisting of sp^2-hybridized carbon atoms which are extremely diverse isometrically and often produce multilayered spherical particles of carbon composed of concentric graphite-like shells called onions. These unique structural features seem to have stimulated the imagination of many scientists, so that their intensive research activities have produced over 20000 papers in a short span of time. A number of encouraging fullerene applications have been suggested since the mid-1990s. Fullerene illustrates the multidisciplinary of nanoscience, involving topics in different fields mentioned here in such as new composite materials for more efficient solar cells, virus inhibition, superconductivity, lithium-ion batteries, drug delivery, nanoelectronics, etc. [19]. All these show the amazing world of carbon and represent the tip of the iceberg of new carbon materials for the 21st century and beyond. However, it would be impossible to analyze in one chapter all of the potential applications mentioned above, so we will focus on some of those which is directly match with this thesis aim.

3.1.1 Structure of fullerene

The C_{60} molecule has been named fullerene after the architect and inventor R. Buckminster Fuller, with designed the geodesic dome that resembles the structure of C_{60}.Orginally the molecule was called buckminsterfullerene, but this name is a bit unwield, so it has been shortened to fullerene. Fullerenes basically are built up of coherent pentagons and hexagons. The pentagons, which are not observed in fullerene allotrope graphite, provide curvature. Buckminsterfullerene has the shape of a soccerball including 12 pentagonal (5 sided) and 20 hexagonal (6 sided) faces symmetrically arrayed to form a molecular ball [18]. In order to close into a spheroid, these geodesic structures must consist of exactly twelve pentagons, but may have a variable number of hexagons (m), with the general composition: C_{20+2m}. Indeed this building principle of the fullerenes is based on consequence of the Euler theorem. In order to account for the bonding of the carbon atoms of a fullerene molecule, the hybridization must be a modification of the sp^3 hybridization of diamond and sp^2 hybridization of graphite [19]. These ball-like molecules bind with each other in the solid state to form a crystal lattice having a face centered cubic structure shown in Fig.3.1. In the lattice each C_{60} molecule is separated from its nearest neighbor by 1 nm (the distance between their centers is 1 nm), and they are held together by weak forces called van der Waals forces [11].

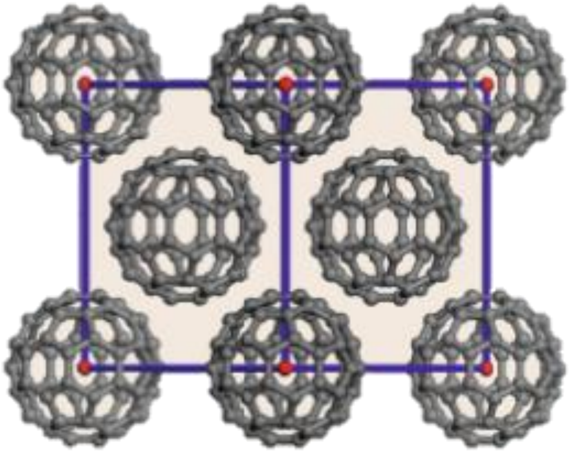

Figure 3.1: The face-centred cubic cell of fullerene C60 [11].

Unlike the sp^3 or sp^2 hybridizations, the fullerene hybridization is not fixed but has variable characteristics depending on the number of carbon atoms in the molecule. This number varies from twenty for the smallest geometrically (but not thermodynamically) feasible fullerene, the C_{20}- to infinity for graphite (which could be considered as the extreme case of all the possible fullerene structures) [15].The fullerene structure is unique in the sense that the molecules are edgeless, chargeless, and have no boundaries, no dangling bonds, and no unpaired electron. These characteristics set the fullerenes apart from other crystalline structures such as graphite or diamond which have edges with dangling bonds and electrical charges. Such features allow these molecules, and particularly the C_{60} which is the most symmetrical, to spin with essentially no restraint at a very high rate [16].

3.1.2 Fullerene production

It has been slightly over ten years since the development of a way to produce macroscopic quantities of fullerene, and the related discovery of fullerene nanotubes. As a result, over 1500 worldwide patents have been filed for the production and applications of these new materials. The family of fullerenes includes the hollow cage all-carbon molecules having a convex closed-shell structure containing arbitrary numbers of hexagonal and exactly twelve pentagonal faces [11, 18]. Most of the methods to produce C_{60} involve very high temperatures (around 4000◦C), such as laser vaporization and arc discharge, because these deal with solid graphite. However, there are other methods which work at lower temperatures such as pyrolysis and electron irradiation, which work with carbon sources that are easier to decompose at lower temperatures. In the case of pyrolysis, an organic compound is used, and in the case of electron irradiation, graphene is used. Certainly, the atmosphere in which the experiments are carried out plays an important role in fullerene formation to avoid undesirable reactions with other elements. To date, the formation mechanisms are not well understood, so different models that have been proposed are reviewed. In this section different methods for obtaining C_{60} and other fullerenes are discussed [19, 20].

3.1.2.1 Arc heating of graphite

In 1990, Arc-Discharge method to synthesize fullerenes was reported by Krätschmer using an electric arc discharge apparatus under a restrictive heating in a helium atmosphere to avoid reactions. This was the first method to produce gram-sized samples. The method was later on modified by Smalley who established an electric arc between two graphite electrodes, where most of the power dissipate in the arc.This modification granted higher yields. Due to these developments a lot of new fullerene families were discovered within the next years[11, 18]. This method could produce a variety of carbon products including high yields of C_{60}, a huge explosion of scientific articles studying its physical and chemical properties.

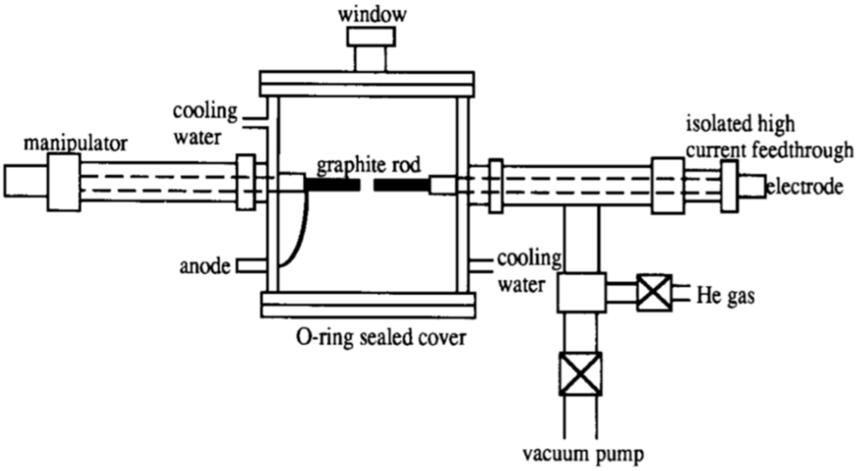

Figure 3.2*:* Schematic illustration of the arc heating apparatus for generating fullerene [20].

A typical fullerene generating apparatus is shown in Fig.3.2. Experiments have been brought out that the most efficient fullerene production operation occurs as the electrodes are barely in contact. This method became the standard to produce higher fullerenes and also carbon nanotubes with low cost [11, 18, 20].

3.1.2.2 Fullerenes by pyrolysis

In the laser irradiation and arc-discharge procedures, it is hard to control and study the fullerene formation process under very high temperatures around 4000◦C. There are a number researches to decrease the temperature and improve control of all the parameters decomposing graphite at lower temperatures. In 1993, C_{60} and C_{70} fullerenes can also be obtained by pyrolysis of hydrocarbons. This method is quite suitable for the preparation of fullerenes because they already comprise fullerene cage structural elements. The first method was the pyrolysis of naphthalene heated about 1000◦C in an argon stream. At these conditions, mainly C_{60} and C_{70} are generated with concomitant cleavage of hydrogen. Synthesis of C_{60} at 700◦C by reduction of CO_2 with metallic lithium has also been achieved [11, 18].

3.1.2.3 Fullerene synthesis in combustion

Another fullerene synthesis method was presented by using flames of hydrocarbons such as benzene. In this method it is possible to provide C_{60} and C_{70} and the ratio of the C_{60}/C_{70} strongly depends on the operation conditions including temperature, pressure, and carbon/oxygen ratio. In further researches put forward higher fullerenes including C_{60} and C_{70} such as C_{76}, C_{78}, C_{80}, C_{84}, C_{86}, C_{88}, C_{90}, C_{92}, C_{94}, C_{96}, C_{98}, C_{100}, C_{102}, and C_{108} in flames of benzene/oxygen/argon at pressures of around 40 Torr [4]. Schematic illustration of the combustion synthesis of fullerenes is presented Figure 3.3. According to 2005 year reports, 400 kg of fullerenes were obtained by this method per year and the amount of this production efficiency will increase as a consequence of further optimizations of the formation of fullerenes in combustion method [11].

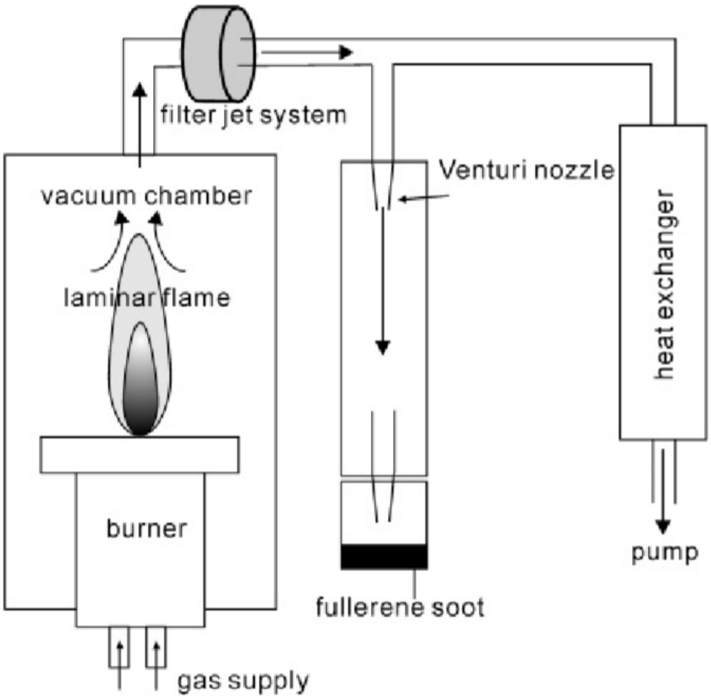

Figure 3.3: Schematic illustration of the combustion synthesis of fullerenes [21].

3.1.2.4 Fullerenes by concentrated solar flux

In concentrated solar flux method, sun light is preferred due to avoid the problem of intense UV-radiation to evaporate graphite the exposure of generated fullerenes to radiation is far less extensive than with arc vaporization techniques. As an example a solar generator called ‘Solar 1’ was developed by Smalley. Basically, this solar generator collects sunlight via a parabolic mirrors and direct this intense sunlight onto a tip of a graphite rod which is mounted inside a Pyrex tube. Besides, the graphite rod was enclosed by helical tungsten preheater in order to minimize conductive heat loss and to provide suitable conditions for the annealing process of the carbon clusters. After the apparatuses and conditions are prepared, the reaction may start easily as the sunlight is focused directly onto the tip of the graphite target. Solar radiation can be concentrated and controlled to build furnaces which can achieve high temperatures (around 3000◦C) and thereby vaporize graphite to form fullerenes. Although this method involves high temperatures as in arc discharge, it can be scaled to increase the yield [11, 18].

3.1.3 Physical properties of fullerene

Fullerenes are extremely strong molecules, able to resist great amount of pressures. Hence, they will bounce back to their initial shape after loaded to over 3.000 atmospheres. Its strength of a chemical bond depends on its bond length. Carbon allotrope, diamond in sp^3-bonded, the C-C bond length is 1.54 Å, while in sp^2-bonded carbon allotrope graphite the in-plane C-C bond length is 1.42 Å. In fact, graphite has an in-plane stiffness is around 1TPa exceeding the corresponding elastic modulus of diamond, 441 GPa. In a C_{60} fullerene molecule, there are two bond lengths (associated with the bond separating two hexagons and bond separating a pentagon and a hexagon); these are 1.46 Å and 1.40 Å. This suggests that an isolated C_{60} molecule might be quite 'stiff'. Theoretical calculations suggest that a single C_{60} molecules is predicted to have an effective bulk modulus of 668 GPa at pressure that makes the 'hard spheres' of C_{60} 'just touch'. These are impressive numbers but they have not been confirmed experimentally [11, 18].

3.2 Graphene Structure and Properties

It was believed that 2D crystals were thermodynamically unstable and could not exist until experimental discovery of graphene, is the two-dimensional allotrope of carbon, consisting of a hexagonal arrangement of carbon atoms on a single plane as shown Figure 3.4. The first isolation of graphene (one atom thick carbon layer) was performed around 2004 by using mechanical exfoliation of graphite, thinning and thinning several times from parent graphite samples. This ground breaking experiments and subsequent investigations into the properties were rewarded with Nobel Prize in physics in 2010.

Remarkable progress has been made in finding out the fundamental properties, exploring the possibility of engineering applications, and growth technologies [22].This chapter explores the history of graphene, as the theoretical building block for other carbon allotropes as well as its rise as a material in its own right in recent years.

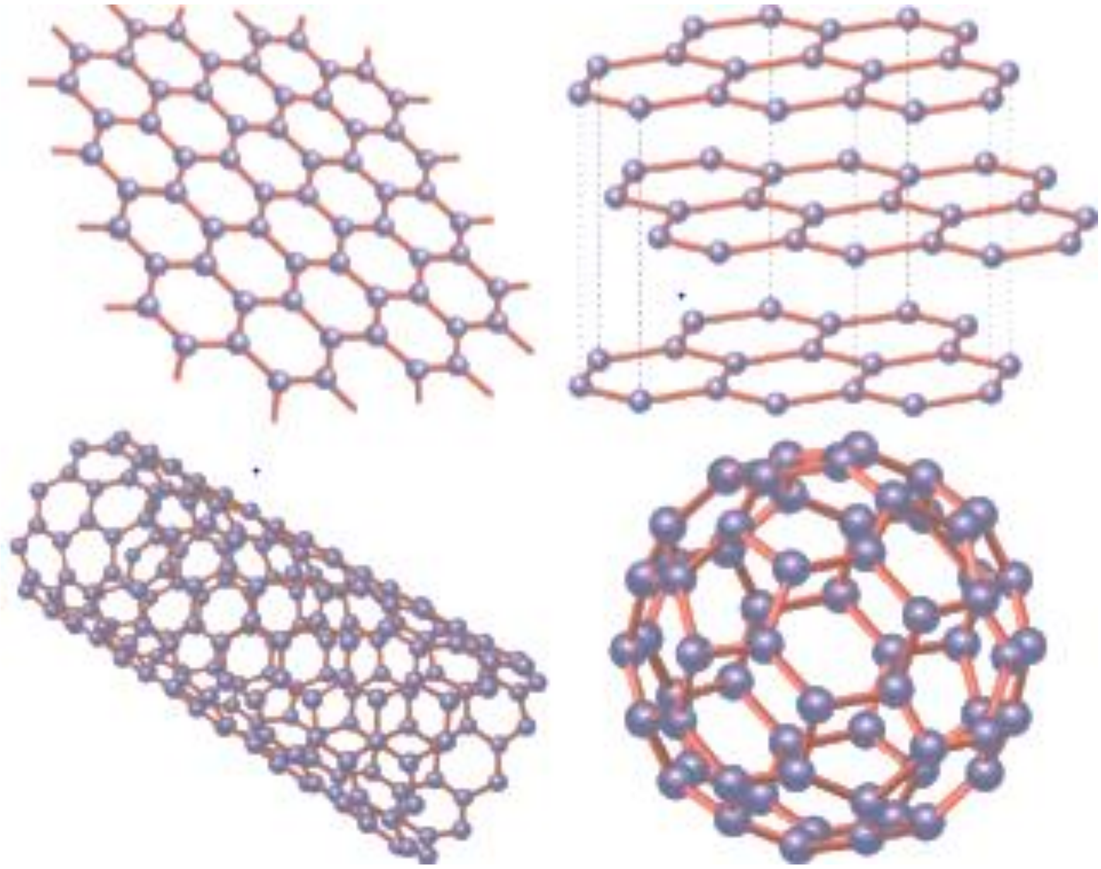

Figure 3.4*:* Graphene based carbon materials. Graphene, Graphite, CNTs and Fullerene [22].

Since its discovery in 2004, graphene has have gained a lot of importance from the scientific community and industry owing to its unequalled electronic, optical, thermal, mechanical, and chemical properties. As a three-dimensional (3D) material, carbon exists as three predominant allotropes: diamond, graphite, and amorphous carbon (historically knows as carbon black). These are distinguished by their crystalline structure and the hybridization of the carbon atoms therein. Carbon atoms in diamond are all sp^3 hybridized and arranged in diamond cubic structure which comprises two interpenetrating face-centred cubic (fcc) lattices. Graphite has a layered structure, where the sp^2 hybridized carbon atoms are arranged in a hexagonal lattice in each plane, while the planes themselves are AB (Bernal) stacked and held together by van der Waals forces. Amorphous carbon, as the name indicates, does not have long-range crystalline order, although locally the atoms are bound together covalently and comprise a mix of sp^2 and sp^3 carbons. While diamond can be reduced in size to the nanoscale to form nanodiamond, it is graphite that can be truly reduced to lower dimensional allotropes [6, 17].

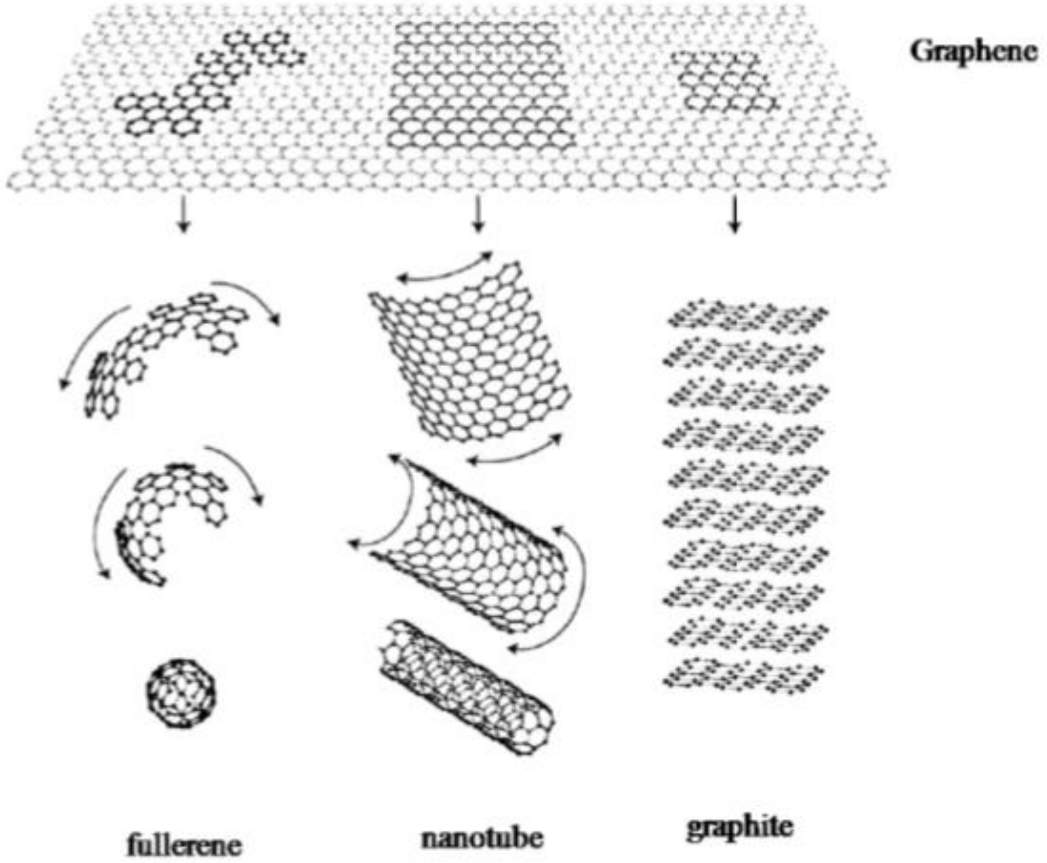

Figure 3.5*:* Graphene is mother of all graphitic forms [23].

A single layer of graphite is defined as graphene is the name given to single thick layer of three-dimensional (3D) graphite forms a two-dimensional (2D) material called 2D graphite or a graphene layer. Graphene is an allotrope of carbon and its structure is one-atom-thick planar sheets of sp^2-bonded carbon atoms tightly packed into a two-dimensional (2D) honeycomb lattice. Graphene is considered as the primal structure for carbon-based materials of all dimensions. Zero-dimensional (0D) fullerenes can be derived from wrapped graphene, (1D) nanotubes can be obtained from rolled graphene and (3D) graphite can be obtained from stacked graphene layers [22, 23].It is demonstrated at Fig. 3.5.

3.2.1 Graphene Production

Graphene can be fabricated by different methods including mechanical exfoliation, chemical vapour deposition, and decomposition of SiC, although bulk-quantity production of pure graphene remains a challenge. The atomic and electronic structure of graphene is described, highlighting the strong correlation in graphene between structure and properties, as is the case with other carbon allotropes. Graphene exhibits a number of unique and superlative electronic and optical properties. The intrinsic properties of graphene can be tailored by nanofabrication, chemistry, electromagnetic fields, etc. Various applications of graphene have been proposed in electronic, optoelectronic, and mechanical products. In addition, graphene has emerged as a candidate in chemical, biochemical, and biological applications [11].Various methods of synthesis and the nature of graphenes are obtained in this chapter.

3.2.1.1 Exfoliation and cleavage

A simply production and low–cost technique is the micromechanical cleavage or exfoliation refers to a peeling operation where graphite sheets are thinned down by mechanically reducing the number of layers in a repeated fashion. Along the interlayer direction graphite layers are held together by weak van der Waals forces, rather than across the strong covalent bonds. Hence, interlayer direction is preferred to peeling operations. The most common procedure to accomplish this is using adhesive tape. There are various type of exfoliation methods such as highly oriented pyrolytic graphite (HOPG), atomic force microscope (AFM), transmission electron microscope (TEM) and graphite oxide (GO) solutions. The first successful thinning down of graphite to its monolayer graphene form involved a wet/dry method. The surface of highly oriented pyrolytic graphite was first patterned into square mesas, which were pressed into wet photoresist. After baking, the mesas attached to the now dry photoresist, and could be detached from the bulk of the HOPG. Another micromechanical cleaving method reported by Ruoff involves the use of an atomic force microscope (AFM) tip along with an array of highly ordered pyrolytic graphite are made from oxygen plasma etching method. The HOPG islands were transferred to a SiO_2/Si substrate using hydrofluoric acid. It is then manipulated using an AFM tip to obtain multiple layers of HOPG. A variation of this method involves gluing a block of prepared graphite to an AFM tip and scratched on Si substrates. In general, it is difficult to control the separation and number of graphene layers generated using these mechanical methods. Another controlled technique to produce few layers of graphene uses a wedge type of tool (generally made with diamond) to address difficulties of the adhesive tape method like low chemical usage and better process controllability. In this method, a sharp single-crystal diamond wedge penetrates onto the graphite source to exfoliate layers. This method uses highly ordered pyrolytic graphite as the starting material. Brittle and hard materials such as germanium have also been sectioned to a nanometer-scale thickness using this technique very recently, Jayasena reported a wedge-based mechanical exfoliation machining technique to produce few layer graphene. An ultra-sharp single crystal diamond wedge is inserted between graphene layers in the highly ordered pyrolytic graphite to cause exfoliation and produce few-layer graphene. Graphite can also be chemically exfoliated in liquid environments exploiting ultrasounds to extract individual layers. [22, 24].

3.2.1.2 Thermal chemical vapor deposition techniques

Deposition of mono-layer graphitic materials on Pt by thermal CVD dates back in 1975.The main objective of this method is preparation and production of large scale and high quality graphene for various applications since the first method in order to produce graphene reported in 2008. In general, thermal chemical vapor deposition (CVD) is a chemical process by which a substrate is exposed to thermally decomposed precursors and the desired product deposited onto the metallic substrate surface at high temperature. There are several metallic substructures have been explored in the effort to grow monolayer graphene. In the early applications, monolayer graphene was grown on Pt (111) by hydrocarbon decomposition at 800◦C, resulting in islands of 20–30 nm size distributed uniformly over the surface. In an attempt to obtain large amount of graphene, regularly shaped, higher temperatures benzene on Ir (111) and graphite on Ni (111) at different environmental conditions and kinetic energy can apply upon annealing process. Graphene has also been grown by thermal decomposition of benzene on Ir (111) and graphite on Ni (111) at different environmental conditions.

There are various experimental setup of CVD. One of the commonly employed method to produce single layer graphene by Cu catalysts is demonstrated schematically at Fig. 3.6. CVD method essentially consist of a furnace for high temperature heating, a quartz vacuum chamber, a vacuum and pressure control system for the growth condition adjustment and several mass flow controllers (MFC) with purpose to supply carbon source and reactant gases with required flow rate. Technological advances in graphene growth by thermal CVD method make reproducibility of high-quality graphene on a centimetre scale possible. The performance of obtained graphene is comparable to that of exfoliated graphene, and these developments provide new routes for large-scale application of graphene. However, the understanding of the optimum growth parameters by thermal CVD is still unclear. Therefore, new approaches beyond existing techniques are necessary for controlling graphene properties and its potential applications [24].

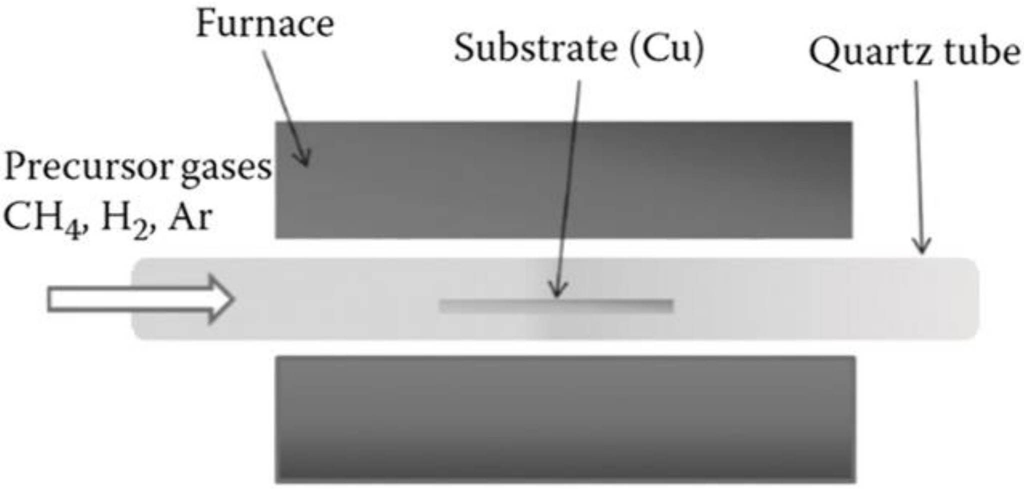

Figure 3.6*:* Schematic of a common setup for chemical vapor deposition of graphene [24].

3.2.1.3 Thermal deposition of SiC

Another method for graphene production is the thermal decomposition of surface layers of single crystal silicon carbide SiC surface which is one of the most widely acclaimed methods of graphene synthesis. Recently, there are 250 different crystal structure of SiC heated to high temperature (>1100 ºC) under low pressure (~10^{-6} Torr) to reduce to graphene. It is known that melting temperature of Si is around 1100 ºC while melting temperature of C is around 3650ºC.This difference between two atoms allows Si atoms selectively sublimate from the surface as SiC is annealed at high temperature. It is firstly showed by Van Bommel in 1975, at higher annealing temperatures in ultrahigh vacuum (UHV), the surface of SiC undergoes various reconstructions, until the graphitization temperature when the surface graphene layers form. A graphene layer grows on hexagonal silicon carbide in UHV at temperatures above about 800ºC.Fig.3.7 shows the schematic of several thermal decomposition of SiC methods for the production of graphene.

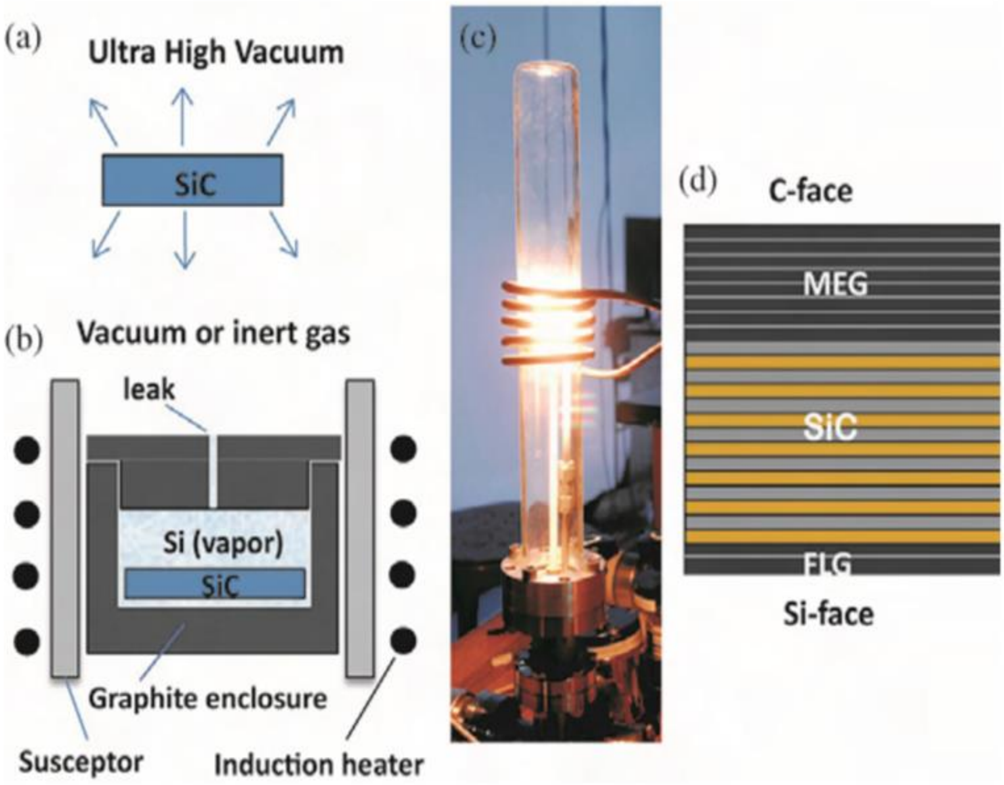

Figure 3.7: Various thermal decomposition of SiC methods for generating graphene.

Many significant graphene properties have been identified in graphene produced by this method, for instance, the electronic band-structure has been first visualized in this material because electronics properties of graphene can control based on fabricating wafer-scale graphene with controlled thickness, width, and specified crystallographic orientations. In addition to controllability of graphene formation, thermal decomposition of SiC methods comprise numerous additional advantages. Firstly, this method requires lower-temperature process than any other methods. Moreover, it is easy that the graphene generated by this process transferred to any substrate for other applications. However, the major advantage of this process comes from is large-scale fabrication of graphene on an insulator or semiconductor surface, which can be used for future complementary metal oxide semiconductor (CMOS)-based electronics. The only major drawback of this method is cost of SiC wafers are relatively expensive than others methods.

The research on thermal decomposition of SiC method for obtaining graphene has attracted huge attention both academically and industrially due to its scalability and production of high-quality graphene. In the light of current researches and knowledge about growth mechanism and the ability to effectively control the number of layers, this method involves enormous opportunities to produce commercially wafer-scale graphene.

3.2.2 Physical properties of graphene

Graphene, an atomic monolayer comprising a hexagonal network of sp^2 bonded C atoms, is the ultimate example of a nanocrystalline material. Graphene, a true two-dimensional crystal, is the basic building block of all graphitic allotropes of carbon found in nature. The carbon atoms are sp^2 hybridized, and the in-plane carbon-carbon bond length is a=1.42Å. The covalently bonded hexagonal network of C-atoms gives graphene a large elastic stiffness and a high elastic strength. Recently measured the ideal fracture strength of single-crystalline graphene using nanoscale indentation and reported an unprecedentedly high intrinsic strength, measuring orders of magnitude greater than those of many conventional materials. In fact, graphene is the only known crystal, which can be stretched in excess of 15%, while remaining in the reversible deformation regime. Graphene is also a promising material because of its ability to be strain-engineered wherein the material properties are tuned by application of a mechanical strain measurements conducted on few-layer graphene of less than 8nm thickness yielded spring constants of 1–5 N/m. A Young’s modulus of 0.5 TPa was extracted by fitting the data to a model for doubly clamped beams under tension. For measurements on monolayer graphene, the force–displacement characteristics yield second and third-order elastic stiffness of 340 N/m and 690N/m, respectively. The breaking strength was found to be 42 N/m, which represents the intrinsic strength of a defect-free sheet. This corresponds to Young’s modulus E =1.0 TPa, third-order elastic stiffness of 2.0 TPa, and intrinsic strength of 130 GPa. These figures mean that graphene is the strongest material ever measured. Nonlinear finite elasticity theory for graphene resonators for both electrostatic and electrodynamic cases has been developed and agrees well with experiments on graphene resonators. A tunable band gap, ultrahigh elastic strength and stiffness, strong adhesion and conformability to complex substrate geometries make graphene desirable for a broad range of micro-nano electromechanical systems. Examples of graphene-based nano-mechanical systems include nanoscale resonators, switches, and valves, with applications ranging from information storage and processing, molecular manipulation, to sensing. Graphene can also be integrated with other microstructures to create a new class of micro-/nano-electro-mechanical devices. In addition to its extraordinary mechanical properties, electronically; monolayer, bilayer, and trilayer graphene are electronically distinct materials. Beyond three layers, graphene’s electronic properties tend towards those of bulk graphite. In certain aspects, graphene of up 10 layers might exhibit deviation in electronic properties from bulk graphite and could be referred to as graphene, but beyond 10 layers, all graphenes are indistinguishable from graphite [11].

4. OVERVIEW OF MOLECULAR DYNAMIC SIMULATIONS

Recent advances in computing technologies in a few decades have significantly increased the interest in computer-based molecular modelling. In the current scientific and industrial world molecular modelling is widely preferred in order to design of new novel material with desirable properties and understand experimental results much more apparently as well.

Fundamentally, molecular dynamics is a technique for computer simulation of complex systems to investigate mechanical behaviour such as stabilities, reactivities and electronic properties at the atomic level. There are various methods and related computer program packages that can be used to calculate to molecular properties. Molecular dynamics (MD) method is one of the well-known approach. This chapter will cover some basic theories of molecular dynamic method and related subjects.

4.1 Introduction to Molecular Dynamics

As the computational power increases day by day, computer methods have become increasingly important in the life sciences because of the complexity of molecular systems. In recent years, modelling methods based on computer simulation have become a beneficial tool in solving numerous scientific and engineering problems. With faster and more powerful computers, larger and more complex systems may be explored using computer modelling or computer simulations in the few years. It is apparent that figure out the equivalent testing in the computer environment is much cheaper than the laboratories. In this aspect molecular dynamics simulations can save significant amount of money in the development stages of novel materials [15].

In history, the progress in science was obtained by real experiments and theoretical work. In an experimental study, the system under investigation is subjected to specific boundary conditions and measurement of parameters that are in question are obtained and numerically stored. In a theoretical work, a physical system is represented by governing mathematical equations consisted of driving parameters of the system. However, theoretical models rely heavily on approximation, both analytical and numerical and are able to be examined only in limited special cases.The stability or predictive capacity of the model should be shown by several simple cases that would allow solvable mathematical equations. For the sake of getting solvable mathematical equations, many times complexities of the system disappears which take us away from the real world problems. Moreover, many of physical issues that fall into the both academic and practical interest, such as physics and chemistry of defects, surfaces, organic molecules and so on, cannot be simplified to be investigated by theoretical models [25].In the light of this information, computer simulation might be preferred which relays on the basic theoretical foundations, in order to try to avoid much of the approximation normally associated with theory, replacing it by a more elaborate calculation effort.

Experimental practice rests on a long (occasionally blemished) tradition; computer simulation, because of its novelty, is still somewhat more haphazard, but methodologies are gradually evolving. If computer resources cannot accommodate this requirement it is presumptuous to expect reliable results. What distinguishes computer simulation in general from other forms of computation, if such a distinction can be made, is the manner in which the computer is used: instead of merely performing a calculation, the computer becomes the virtual laboratory in which a system is studied a numerical experiment. The analogy can be carried even further; the results emerging from a simulation may be entirely unexpected, in that they may not be at all apparent from the original formulation of the model.

This brief discussion illustrates that very often there is not enough information to link theory and experiment. Thus, analytical approximations involved in the description of an experimentally observed phenomenon are not necessarily related to the real driving forces of this phenomenon. Computer-based modeling methods provide a unique opportunity to build a "coherence bridge" between the analytical approximations involved in the solution of major problems and the experimental information available.

Molecular dynamics is a technique for computer simulation of complex systems, modelled at the atomic level. The equations of motion are solved numerically to follow the time evolution of the system, allowing the derivation of kinetic and thermodynamic properties of interest by means of ‘computer experiments’. There are two main families of MD methods, which can be distinguished according to the model (and the resulting mathematical formalism) chosen to represent a physical system. In the ‘classical’ mechanics approach to MD simulations molecules are treated as classical objects, resembling very much the ‘ball and stick’ model. Atoms correspond to soft balls and elastic sticks correspond to bonds. The laws of classical mechanics define the dynamics of the system. The ‘quantum’ or ‘first-principles’ MD simulations, which started in the 1980s with the seminal work of Car and Parinello, take explicitly into account the quantum nature of the chemical bond. The electron density function for the valence electrons that determine bonding in the system is computed using quantum equations, whereas the dynamics of ions (nuclei with their inner electrons) is followed classically. Quantum MD simulations represent an important improvement over the classical approach and they are used in providing information on a number of biological problems. However, they require more computational resources [25].

The most prominent advantage that the MD simulations provide to researchers is the extraction of all properties about a thermodynamic system which is physically possible to exist. Especially in a conceptually difficult field such as physics, simulation can be used to help overcome some of the more counter intuitive concepts encountered even at a relatively elementary level. Simulation plays an important role in education. It takes little imagination to see how interactive computer demonstrations of natural phenomena can enrich any scientific presentation. As to the role of MD, it can bring to life the entire invisible universe of the atom, an experience no less rewarding for the experienced scientist than for the utter tyro. But, as with education in general, simulation must be kept honest, because seeing is believing, and animated displays can be very convincing irrespective of their veracity. However, the power of the MD is limited to computational power and time-scale range that can be covered [15]. Theoretically, molecular structure of a material, which may be organic or inorganic, can be designed in a numerical environment and its material properties can be determined via computer simulation methods such as the MD simulations. By using numerical specimens with different molecular structures, an optimum molecular structure that satisfies required material properties can be obtained. Following these numerical design iterations, proposed material can be synthesized in the laboratory and further refinements can be done in the laboratory environment [15]. From this point of view, molecular dynamics simulation method holds very important step to be taken towards novel materials or nano electromechanical device design. While its usage currently is limited to academic field excluding a few areas such as pharmaceutical and polymer design, in the next 20 years the MD simulation technique is estimated to take the place of today's computational tools, e.g., CFD or FEM in industry [15].

4.2 Historical Background

There is a complex network of chemical entities that evolve dynamically creating life at the molecular level. For example, proteins and nucleic acids fold (adopting specific structure consistent with their function), ions are transported through membranes, enzymes trigger cascades of chemical reactions, etc. Because of the complexity of biological systems, computer methods have become increasingly important in the life sciences. With faster and more powerful computers larger and more complex systems may be explored using computer modelling or computer simulations. Molecular dynamics (MD) emerged as one of the first simulation methods from the pioneering applications to the dynamics of liquids by Alder and Wainwright and by Rahman in the late 1950s and early 1960s. Due to the revolutionary advances in computer technology and algorithmic improvements, MD has subsequently become a valuable tool in many areas of physics and chemistry. Since the 1970s MD has been used widely to study the structure and dynamics of macromolecules, such as proteins or nucleic acids.

The 'quantum' or 'first-principles' MD simulations, which started in the 1980s with the seminal work of Car and Parinello, take explicitly into account the quantum nature of the chemical bond. The electron density function for the valence electrons that determine bonding in the system is computed using quantum equations, whereas the dynamics of ions (nuclei with their inner electrons) is followed classically. Quantum MD simulations represent an important improvement over the classical approach and they are used in providing information on a number of biological problems. However, they require more computational resources [25].

4.3 Molecular Dynamics Foundation

Molecular dynamics simulation provides the methodology for detailed microscopic modelling on the molecular scale. The theoretical basis for MD embodies many of the important results produced by the great names of analytical mechanics – Euler, Hamilton, Lagrange, and Newton. Their contributions are now to be found in introductory mechanics texts. Some of these results contain fundamental observations about the apparent workings of nature; others are elegant reformulations that spawn further theoretical development. The simplest form of MD that of structureless particles, involves little more than Newton's second law. Rigid molecules require the use of the Euler equations, perhaps expressed in terms of Hamilton's quaternions. Molecules with internal degrees of freedom, but that are also subject to structural constraints, might involve the Lagrange method for incorporating geometric constraints into the dynamical equations. Normal equilibrium MD corresponds to the microcanonical ensemble of statistical mechanics, but in certain cases properties at constant temperature (and sometimes pressure) are required; there are ways of modifying the equations of motion to produce such systems, but of course the individual trajectories no longer represent the solution of Newton's equations. The equations of motion can only be solved numerically. Because of the nature of the interatomic interaction, exemplified by the Lennard-Jones potential with a strongly repulsive core, atomic trajectories are unstable in the sense that an infinitesimal perturbation will grow at an exponential rate, and it is fruitless to seek more than moderate accuracy in the trajectories, even over limited periods of time. Thus a comparatively low-order numerical integration method often suffices; whether or not this is adequate emerges from the results, but the reproducibility of MD measurements speaks for itself. Where softer interactions are involved, such as harmonic spring sort or sional interactions, either or both of which are often used for modelling molecules with internal degrees of freedom, a higher-order integrator, as well as a smaller time step than before, may be more appropriate to accommodate the fast internal motion. The numerical treatment of constraints introduces an additional consideration, namely that the constraints themselves must be preserved too much higher accuracy than is provided by the integration method, and methods exist that address this problem [26].

Rather than attempting to deduce microscopic behaviour directly from experiment, the molecular dynamics method follows the constructive approach in that it tries to reproduce the behaviour using model systems. The continually increasing power of computers makes it possible to pose questions of greater complexity, with a realistic expectation of obtaining meaningful answers; the inescapable conclusion is that MD will, if it hasn't already, become an indispensable part of the theorist's toolbox.

Applications of MD are to be found in physics, chemistry, biochemistry, materials science, and in branches of engineering.

4.3.1 Basic theory

In MD simulations the time evolution of a set of interacting particles is followed via the solution of Newton's equations of motion, eqn (3.1), where $r_i(t) = (x_i(t), y_i(t), z_i(t))$ is the position vector of ith particle and F_i is the force acting upon ith particle at time t and m_i is the mass of the particle.

$$F_i = \frac{d^2 r_i(t)}{dt^2} \tag{4.1}$$

As a common approach the simplest MD codes require basically three information to integrate the above second order differential equations how the particles interact with each other, initial position of the particles and the initial velocities of the particles. The MD trajectories are defined by both position and velocity vectors and they describe the time evolution of the system in phase space. In MD simulations, there are several numerical algorithms, which can be used to integrate equation of motion. As a one of the most popular numerical integrators, Verlet, defines the position of each particle in space is defined by r(t), whereas the velocities v (t) determine the kinetic energy and temperature in the system as follows:

$$v\left(t+\frac{dt}{2}\right) = v(t) + a(t)\frac{dt}{2} \tag{4.2}$$

$$r(t+dt) = r(t) + v\left(t+\frac{dt}{2}\right)dt \tag{4.3}$$

$$a(t+dt) = \ddot{r}(t+dt) = F\left(r(t+dt)\right) \big/ m \tag{4.4}$$

$$v(t+dt) = v\left(t+\frac{dt}{2}\right) + \frac{1}{2}\left(a(t+dt)\right)dt \tag{4.5}$$

Where a is the acceleration t is time and F is force. The advantages of using the velocity Verlect algorithm is that the velocity term appears directly in the equation of motion to be iterated, so that no extra effort or storage is required. Apart from that, the equation retain the superior numerical precision of the summed form.

The aim of the numerical integration of Newton's equations of motion is to find an expression that defines new positions of the each particle in terms of the already known positions at time *t*. Applying the Newton's second law to the forces on each particles provides the particle's acceleration '**a**' as expressed at equation (4.6).

$$a = F/m \tag{4.6}$$

In the light of this information the initial velocity of each particle can be used to calculate the particle's new position after applying a small time step dt .Verlet algorithm is widely preferred in MD simulations and the basic formula derived from the Taylor expansions for this algorithm for the positions $r_i(t)$ can be expressed as in eqn (3.7).

$$r_{t+\mathrm{d}t} = r_t + v_t \mathrm{d}t + \frac{1}{2} a + (\mathrm{d}t)^2 \tag{4.7}$$

The subscripts t and t + dt denotes the value before and after the time step, respectively. The new velocity is

$$v_t = v_t + a\mathrm{d}t \tag{4.8}$$

The positions and velocities after the next time step is calculated using the updated positions and velocities, r_{t+dt} and V_{t+dt}. The process is repeated until the required number of steps have been performed to give the total simulation time. Equations (4.6) and (4.7) are the Euler integration method, the simplest time-integration method for updating atomic positions and velocities from one time step to the next. In most time integration methods, the acceleration is constant during each time step. At small enough time steps, this is a satisfactory approximation. However, each time step uses values from the previous time step so errors accumulate and can be quite large by the end of the simulation. More sophisticated codes will calculate velocities and positions with different integration methods to minimize the error associated with the choice of dt.

4.3.2 MD limitations

Despite of the attractive possibilities provided by the MD method that helps researcher to dive into the atomistic world, MD is not without limitations. There are some limitations that need to be addressed. Basically, the two main constraints of this method on the MD come from the time and length scales of process. The time limitation is the most severe problem in MD simulations. The fastest motion in the system, typically the atomic vibrations, limit the maximum time step that can be used. A typical MD time step is around 1 fs and current computational capabilities limits the total number of time steps to 10^6 – 10^8 so the total simulation time is limited to around 100 ns. Available computational capabilities also limit the maximum system size. Typical simulations can contain 10' to 10^8 particles, corresponding to a system size of 1 nm to 100 nm.

The main framework of molecular dynamics basically include three basic steps form. In the first step, initial positions and velocities for each atom in the system are assigned. Then, the particles in the simulation box commenced to interact with each other via a potential function and forces acting upon each atom are calculated based on the potential used. For this reason, another issue with the MD simulations is the calculation of forces. It will not be wrong to state that the degree of realism of the MD simulation highly relies on the capacity of the potentials to capture the same response of the material under the boundary conditions that are employed in the simulation. Because the interaction between atoms results in the forces acting upon corresponding atoms, which drive the motion of the atoms in the system, calculation of forces on the atoms as accurate as is very important to capture the real physical response. Due to computational efficiency, potential calculations are not performed between all atoms. Instead of that, by defining a radius of neighbourhood, for each atom, only a number of atoms within the neighbourhood are used to determine interatomic forces.

5. MODEL GENERATION

The aim of this thesis to investigate mechanical properties of the novel fullerene-graphene nano-foam. Up to now, detailed information about carbon nanostructures and brief introduction of the molecular dynamic simulations are introduced. In this chapter, all steps of creating a molecular dynamic model are captured apparently. Firstly, brief information about capabilities of the selected molecular dynamic simulation programme. Then, it will be mentioned about all phases of the model creation. Besides, required theoretical information and equations are obtained in order to understand the nature of the molecular dynamic simulations. After a detailed explanation about model creation, finally, overall options of classical molecular dynamic simulation are collected and summarised.

5.1 Lamps Script Generation and MD Model Creation

In this thesis, simulations were performed using the 16 February 2016 release of LAMMPS "Large-scale Atomic/Molecular Massively Parallel Simulator" - a classical MD program from Sandia National Laboratories. LAMMPS is an open source software supporting a molecular dynamics simulation package [27]. Various types of systems can be simulated, e.g. atoms, polymers, biological molecules, metallic particles, granular and coarse-grained systems and their transport properties can be observed in solid, liquid or gas states. Moreover, serial or parallel simulations can be run from a single script, which can considerably reduce the time requirement of certain simulations.

Essentially, two main inputs are required in LAMMPS: (1) An input data file containing information about atom types, initial coordinates, bonds, angles, dihedral and improper quadruplets and (2) an input script has been writing using LAMMPS code. A LAMMPS input script is sub-divided into six parts for this specific study: initialization, atom definition, force field definition, minimization phase, equilibration phase and deformation phase.

5.1.1 Initialization phase

In this part of the input data analysis parameters need to set before atoms read from input file. These parameters particularly comprises dimension, boundary, atomic style and units definitions. In this study for each case the parameters are set as shown below;

```
# ---------- Initialize Simulation -------------------
dimension 3
boundary   p p p
atom_style atomic
units metal
neighbor 2.0 bin
neigh_modify every 1 check no
# ---------- Initialize Simulation -------------------
```

The ¨*dimension*¨ command sets the dimensionality of the simulation regarding to run 2D simulation or 3D simulation. In this study, dimensions are set ¨*3*¨.

One of the crucial computational parameter on the molecular dynamics simulations is the boundary condition. The ¨*boundary*¨ command specifies the boundary conditions for the global simulation box in each dimension. In order to compute bulk properties, it is required to simulate infinitely extended systems to avoid surface effects. This is accomplished by imposing ¨*periodic*¨ boundary condition is applied means the "*p p p*" style is chosen, indicating that the box is periodic in the x, y and z dimensions.

The periodic conditions can be applied to the boundaries in specific directions assumed to be in the infinite bulks. Conceptually, the simulation box is repeated infinitely in all intended directions in the periodic boundary conditions and if some atom exit one end of the current simulation box, another atom having the same velocity re-enters from the end of simulation box. Figure 5.1 represents the periodic boundary condition mechanism. This is very useful to describe the bulk systems of materials. However, there is some restrictions in which periodic boundary conditions can not be used, for instance, if the surface effects are of particular interest, the periodic boundary conditions should not be applied to the directions.

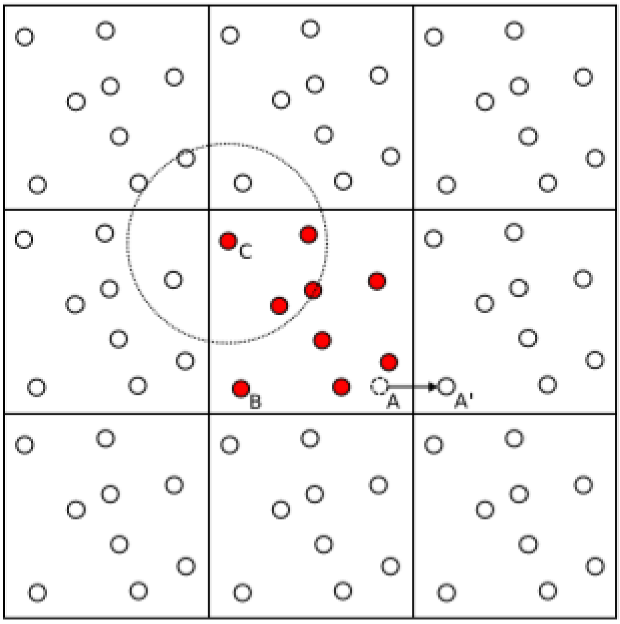

Figure 5.1: Periodic boundary conditions. The atom at A, when moving to the position A^I outside the central simulation box, will instead be translated at B. All the atoms and periodic images of atoms interacting with atom labeled C are shown inside the big dotted circle [25].

In order to determine what type of attributes are associated with the created atoms and what quantities are computed and listed in the data file, ¨*atom_style*¨ command is used [27].In this specific study ¨*atomic*¨ style is chosen to store quantities of the model throughout the simulation.

The ¨*units*¨ command is applied with intent to set the style of units for the simulation. It specifies the units of all the quantities defined in the input script and data file, as well as quantities output to the screen, log file, and dump file. Specific to this study, the "*units*" style chosen is ¨*metal*¨ which uses conventional MD units [27]:

- mass = grams/mole
- distance = Angstroms
- time = picoseconds
- energy = eV
- velocity = Angstroms/picosecond
- force = eV/Angstrom
- torque = eV
- temperature = Kelvin

- pressure = bars
- dynamic viscosity = Poise
- charge = multiple of electron charge (1.0 is a proton)
- dipole = charge*Angstroms
- electric field = volts/Angstrom
- density = gram/cm^dim

In the molecular dynamics simulations, the current atomic position and velocity are employed by solving the systems of the differential equations for each timestep. In the computer simulations of molecular dynamics, most computational resources are spent in calculating the interatomic potential energy given at the atomic configurations, and the interatomic potential energy vanishes rapidly as the interatomic distance increases. Therefore, it is impossible and inefficient to calculate all the interactions in the system for each time. That is, we need to calculate the interatomic potential energy or force of the system based on the nearest neighbor atoms which contribute the energy or force significantly. To realize this, we need to construct the neighbor lists of atoms in the system during the simulations. The most popular and simplest neighboring scheme in the molecular dynamics is to track and store neighbor atoms on each atom during the simulations. In this method, the neighbor list of the atoms is constructed based on the atomic distance within the proper cutoff radius. That is, for a specific atom, all the atoms within the cutoff radius from the central atom are stored in the neighbor list for the atom. The ¨*neighbor*¨ command set the parameters which affect the building and use of pairwise neighbor lists. It is not efficient way to construct the neighbor lists for all atoms in the system every single step. Hence, in the practical simulations, organizing the neighbor lists according to a cutoff distance is an effective way obtaining computational efficiency. As a consequence of this approach, all atom pairs within a neighbor cutoff distance equal to their force cutoff plus the skin distance are stored in the neighbor list. In this study, 2 A cutoff distance is employed respect to default metal unit advice [27]. Figure 5.2 demonstrates cutoff distance and neighbor lists.

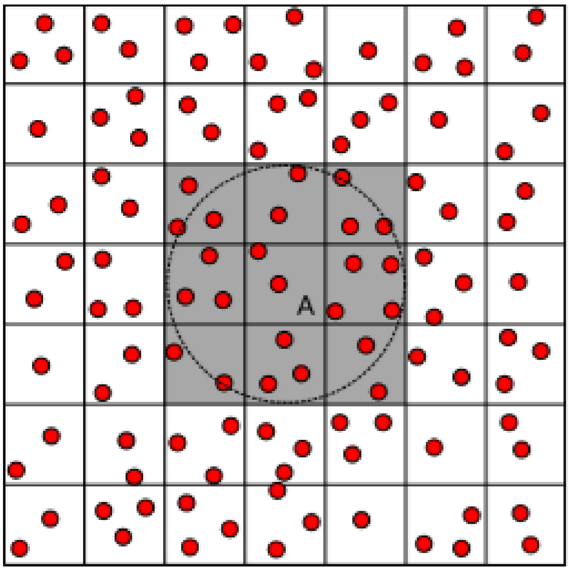

Figure 5.2: Link-cell algorithm in two dimensions. To compute the interactions with the atom labeled A, all the atoms inside the same sub-cell as A are considered, as well as all the atoms in the adjacent sub-cells within the cutoff radius [25].

In molecular dynamics simulations, various neighboring styles give same results under the same conditions while choosing the neighboring style and frequency influence on the computational efficiency. The ¨bin¨ style is preferred in this study due to its faster algorithm than any other style under neighbor command such as ¨nsq¨ style. Another parameter frequency is controlled by ¨neigh_modify¨ command. The arguments for "neigh_modify" are set “every 1 check no", which instructs LAMMPS to build the neighbor list on every step and the lists are built on the first step that satisfies the delay and every settings [27].

5.1.2 Atom definition phase

In the parallel of the main objective of this study, we consider a model comprised fullerenes sandwiched graphene flakes. Essentially, randomly and evenly distributed fullerenes (C_{180} size) composite structures are generated on the purpose of investigating the effects of spatial distribution of fullerenes on the mechanical behaviours. Some control parameters are defined to manage fullerene arrangement on graphene layers. Primarily, a strict distance control is imposed to prevent possible intersection problems of the fullerenes located on the same graphene sheet for both randomly and ordered distributed models while the locations of the fullerenes are determined randomly. As a secondary control rule for randomly distributed model, a fullerene on a single graphene sheet are arranged in a way that a fullerene on a layer does not coincide with any other fullerene positioned on the lower and upper neighbour layers for randomly fullerene located models as illustrated Figure 5.3 and cross-section of the randomly fullerene model is presented as shown in Figure 5.4 (d).In addition to randomly fullerene distributed model, hexagonal, square and rotated-hexagonal ordered fullerene-graphene nano composite models are generated and their cross-section (top view) are presented in Figure 5.4 (a) , Figure 5.4 (b) and Figure 5.4 (c) respectively. Another control parameter is defined for rotated-hexagonal model. In accordance with this control parameter, fullerenes are located on graphene sheets hexagonally and this structure is rotated 60° in each graphene-fullerene layers respect to graphene sheet center additionally.

The lengths of the graphene sheets are 20 nm in two directions and the total area of the graphene sheet is 400 nm^2 and approximate radius of chosen fullerene, which are C_{180}, are 0.6 nm. All models comprise 11 graphene sheets and 10 sandwiched layers. Number of fullerenes between two graphene layers are kept constant for all models individually while as a consequence of different fullerene arrangement on graphene sheets, the number of fullerenes are variable among four models. However, fullerene density of the models is tried to keep constant with only % 1 difference in same fullerene type located on graphene flakes.

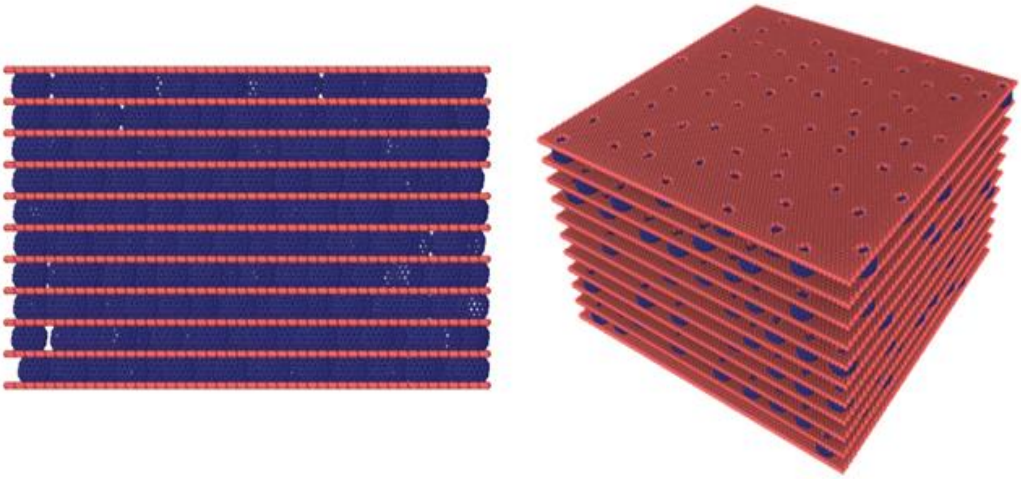

Figure 5.3: Randomly fullerene distributed atomistic model of nano-sandwiched foam.

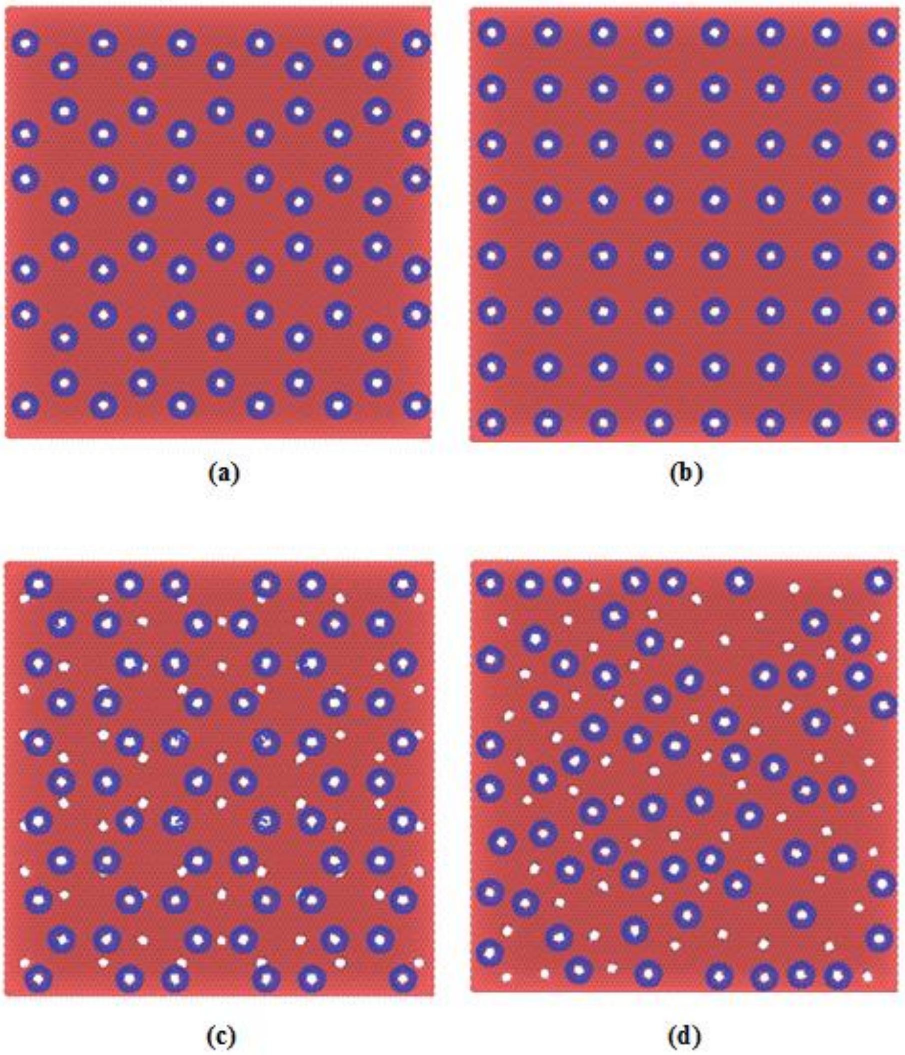

(a) (b)

(c) (d)

Figure 5.4: Cross-sections (top views) of randomly and evenly generated fullerene-graphene composite specimens: (a) Hexagonal arrangement (b) Square arrangement (c) Rotated-Hexagonal arrangement (d) Random arrangement.

All atoms coordinates are defined by using corresponding 'Matlab' script ,which is presented attachment, and imported to LAMMPS environment by using '*read_data'* and '*include*' commands as expressed below;

```
# ---------- Atom Definition----------------

read_data graphene_welding.dat

include include.dat

# ---------- Atom Definition----------------
```

5.1.3 Force field definition phase

In the molecular dynamics simulations, we obtained the current atomic position and velocity by solving the systems of the differential equations. In the computer simulations of molecular dynamics, most computational resources are spent in calculating the interatomic potential energy given at the atomic configurations, and the interatomic potential energy vanishes rapidly as the interatomic distance increases. The interatomic potential energy of the system is calculated from the interatomic force fields for the system based on the current atomic configurations. In terms of the interacting forces acting on atoms, the interatomic potential function is the most important in the molecular dynamics simulations. Currently, there are many potential functions for materials. In the early stage of the molecular dynamics simulations, one of the simplest, a pairwise interaction function was developed to describe the interacting monatomic gases and solids. As pairwise interactions, various Lennard Jones (9-3 or 12-6) potentials have been developed for many material systems. As the Lennard Jones potentials are relatively simple to implement, they are still used in many material systems.

5.1.3.1 Lennard-Jones potential

Lennard-Jones potential whose formulation is given below is one of the most well-known potential utilized for Van der Waals system and initially offered to be used for Argon (see Figure 5.5).

$$u_{LJ}\left(r_{iJ}\right)=4\varepsilon\left[\left(\frac{\sigma}{r_{iJ}}\right)^{12}-\left(\frac{\sigma}{r_{iJ}}\right)^{6}\right] \qquad (5.1)$$

Lennard-Jones potential is especially suitable for closed-shell materials such as Neon and Argon liquids where the electrons are confined to each atomic nucleus; therefore, for open-shell systems where strongly localized bonds are observed; it is not fully satisfactory.

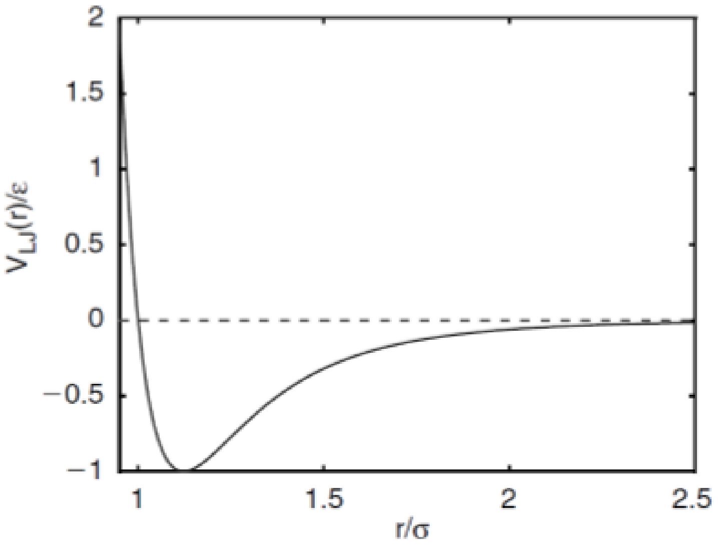

Figure 5.5: Lennard-Jones potential.

5.1.3.2 AIREBO potential

Adaptive Intermolecular Reactive Empirical Bond Order potential (AIREBO) for hydrocarbons has been widely used to study dynamic bonding processes under ambient conditions. However, its intermolecular interactions are modelled by a Lennard-Jones (LJ) potential whose unphysically divergent power-law repulsion causes AIREBO to fail when applied to systems at high pressure. The adaptive intermolecular REBO (AIREBO) potential was developed by Stuart, Tutein and Harrison based on the second-generation REBO potential, although it was published earlier. The potential aims at improving a description of non-bonded interactions in the systems where they play a key role, liquid and amorphous solids and graphite. It has been applied to study compressed CNT filled with C_{60} (buckminsterfullerene) molecules, the stress-induced warping of graphene sheets and nanoribbons. To take into account the non-bonded interactions, a long-range Lennard-Jones (LJ) potential is added to the total energy calculation.

5.1.4 Minimization phase

After the appropriate system size definition and atom generation, the next step is to identify a reasonable "*timestep*" and "*minimize*" the energy within the system. The value for the timestep size depends on the model type and choice of units for the simulation. In specific to these analysis timestep is set "*0.001*" picosecond as shown below;

```
# ---------- Minimization --------------------
timestep          0.001
minimize 1e-6 1e-6 1000000 1000000
# ---------- Minimization --------------------
```

Perform an energy minimization of the system, by iteratively adjusting atom coordinates. Iterations are terminated when one of the stopping criteria is satisfied. At that point the configuration will hopefully be in local potential energy minimum. Typically, the initial atomic structure used in the calculations is not actually the optimal stable structure, but a guess at what that structure would be. Therefore, the stable structure must be found by allowing the atoms to move to more stable (i.e. lower energy) configurations. Minimization, by itself, provides a great deal of information about the system. When starting calculations for system dynamics, however, it is imperative to first find a minimum in the energy surface to serve as a stable starting point. The minimized system is the configuration about which fluctuations occur during the time trajectory of the system. The fluctuations, in turn, provide the dynamics that are the underpinning of MD. The net force on each atom is zero at a minimum energy point, and a system may have more than one local minimum. Typically, the local minimum can be found easily by using well-developed protocols, but finding the global minimum requires a scan of the conformational space

For an MD system, there are many more degrees of freedom and additional complexities, but the principle is the same as this example. Energy minimization algorithms are typically built into MD software, as is the case for LAMMPS, since they are vital to the simulation; all the user has to do is call up the appropriate commands in the input script.

5.1.5 Equilibration phase

Once a local minimum energy configuration has been found, the work of creating a statistically accurate MD representation of the system under investigation can begin in earnest. The next step is equilibrating the system to reach the desired temperature and pressure conditions through use of a thermostat or barostat. In addition to randomizing molecule locations, equilibration serves the more important purpose of properly distributing the total energy between potential, kinetic, and adjusting energies within the system to maintain the desired temperature or pressure even when thermostats and barostats are removed from the equations of motion.

The basic MD formulation is a description for the microcanonical ensemble: the system is completely isolated. In MD, the microcanonical ensemble is often called the NVE ensemble, where N refers to the number of atoms, V to the volume of the system, and E to the total system energy, since N, V, and E are held constant. However, most physical systems are not isolated. Instead, typically either the temperature and/or pressure is held constant instead of the total energy. These are the NVT and NPT ensembles, respectively. Thermostats and barostats required in NVT and NPT ensembles to maintain the desired temperature and/or pressure.

The expression for system temperature in equation (4.1) suggests a simple way to maintain a constant temperature. At each time step, the velocities of the atoms can be rescaled by multiplying each velocity with a factor λ. This procedure produces the desired temperature as;

$$
\begin{aligned}
T_d &= \frac{1}{3Nk_B}\sum_{i=l}^{N} m_i\left(\lambda v_i\right)^2 \\
&= \frac{\lambda^2}{3Nk_B}\sum_{i=1}^{N} m_i v_i^2 \\
&= \lambda^2 T \\
\lambda &= \sqrt{\frac{T}{T_d}} \qquad (5.2)
\end{aligned}
$$

where T is the temperature before rescaling. If the temperature is too high, this method takes some energy out of the system by slowing all the atoms down, and if the temperature is too low, this method adds energy by increasing the velocities. This rescaling enforces the desired temperature at every time step so that if the desired temperature is far away from the current system temperature, rescaling by λ will introduce large temperature fluctuations accompanied by large over or under shooting. Furthermore, this rescaling does not allow for any fluctuations in system temperature, which may not be physical.

The Berendsen thermostat solves much of the issues with the velocity rescaling method by changing the velocity slowly over many time steps such that

$$\frac{\mathrm{d}T}{\mathrm{d}t}=\frac{1}{\tau}\left(T_{\mathrm{d}}-T\right) \tag{5.3}$$

where τ controls how quickly the temperature is changed. The change in temperature at each time step is

$$\delta T=\frac{\delta t}{\tau}\left(T_d-T\right) \tag{5.4}$$

where δT is the size of the time step. Then, the required velocity scaling parameter

$\lambda_{Berendsen}$ is calculated as

$$\delta T=\lambda_{Berendsen}^{2}T-T=\frac{\delta t}{\tau}\left(T_d-T\right) \tag{5.5}$$

$$\lambda_{Berendsen}=\sqrt{1+\frac{\delta t}{\tau}\left(\frac{T_d}{T}-1\right)} \tag{5.6}$$

Note that if $\tau=\delta t$, $\lambda_{Berendsen}$ reduces to the simple rescaling parameter in equation (4.2) and the Berendsen method becomes the simple velocity rescaling discussed previously. In contrast, as $\tau \rightarrow \infty$, $\lambda_{\mathrm{Berendsen}} \rightarrow 1$ so the velocity is no longer being rescaled and the system reduces to the microcanonical ensemble.

The pressure of the system can be calculated from;

$$P=\frac{Nk_BT}{V}+\frac{\sum_i^N r_i f_i}{\mathrm{d}V} \tag{5.7}$$

where P is the system pressure, V is the system volume, r_i is the position of the i_{th} atom, f_i is the force on the ith atom, and d is the number of dimensions in the system. For a bulk system, $d = 3$. Note that the first term of equation is the familiar ideal gas law and the second term is a viral correction to account for atom interactions. Similarly, to temperature, the expression for pressure suggests a simple way to adjust the system pressure during calculations: by changing V. The system volume can be adjusted by length scaling to change the system pressure, P, to the desired pressure, $P_{desired}$, similar to scaling the atom velocity to change the system temperature. For a cubic system, the volume of the system and the length of the system, l, is related by $V=l^3$, so the scaling becomes

$$V = l^3 \rightarrow \mu^3 l^3 \tag{5.8}$$

$$r_i \rightarrow \mu r_i \tag{5.9}$$

As in thermostating, the Berendsen method provides a way of slowly adjusting the volume towards the desired pressure. The Berendsen scaling factor is

$$\mu_{Berendsen} = \left[1 - \frac{\beta \delta t}{\tau_p} \left(P_d - P \right) \right] \tag{5.10}$$

where β is the isothermal compressibility. This choice for scaling factor satisfies

$$\frac{dP}{dt} = \frac{1}{\tau_p} \cdot \left(P_d - P \right) \tag{5.11}$$

isothermal compressibility for the system is not required to apply the Berendsen barostat since β appear only in a ratio to τ_p, the pressure relaxation timescale.

The Berendsen thermostat in conjunction with the Berendsen baraostat give realistic fluctuations in temperature and pressure and are extremely efficient for relaxing the system to the desired temperature and pressure. However, they do not produce canonical distributions. Other methods, notably Nose-Hoover, have been developed and proven to accurately reproduce equilibrium canonical statistics. The Nose-Hoover thermostat changes the equations of motion to include a heat bath that is used to maintain the system at the desired temperature. Then, the extended system (heat bath and original system) forms a microcanonical ensemble while the original system correctly produces equilibrium canonical behavior. Since the Green-Kubo formulas are derived under the assumption of canonical ensembles, the Nose-Hoover thermostat is often used to enforce an NVT ensemble during the production run. However, the Nose-Hoover thermostat has only been proven to produce the correct equilibrium canonical statistics, and no thermostat has been proven to produce the correct dynamical properties, such as the heat flux correlation functions used in the Green-Kubo method. Instead, the heat flux correlation functions should be evaluated by averaging multiple NVE runs from systems that have been carefully relaxed to equilibrium in NVT.

Every time the system temperature and pressure is adjusted through the thermostats, the system will be out of equilibrium. Additional time steps are required to bring the system back into equilibrium. Note that this equilibrium refers to the dynamic equilibrium, not the minimum energy equilibrium configuration found during minimization. A well equilibrated system will keep fairly constant pressure and temperature even without additional constraints from thermostats and barostats. This allows an NVE ensemble to produce the canonical distributions required for Green-Kubo. It is a good practice to switch between NVT and NPT ensembles several times during equilibration and, before starting the production run, to confirm that the system is indeed well equilibrated with a NVE equilibration segment.

5.1.6 Deformation phase

After obtaining stable equilibration for graphene-fulerene nano-foam models, uniaxial compressive loading is employed by using LAMMPS ‘erate’ command. The erate style changes a dimension of the the box at a “constant engineering strain rate”. The units of the specified strain rate are 1/time. Tensile strain is unitless and is defined as delta/L_0, where L_0 is the original box length and delta is the change relative to the original length. The box length L as a function of time will change as

$$L_{(t)} = L_0 \, (1 + \mathrm{erate}{*}d_t) \tag{5.12}$$

where dt is the elapsed time (in time units). Thus if erate R is specified as 0.1 and time units are picoseconds, this means the box length will increase by 10% of its original length every picosecond.

5.2 Overall Simulation Options and Scope of MD Simulations

This section describes the procedure for preparing representative MD model in order to simulate mechanical behavior of novel hybridized carbon-based material. Simulations were carried out by using Large-scale Atomic/Molecular Massively Parallel Simulator (LAMMPS) and Open Visualization Tool (Ovito) software packages. Basically, molecular calculations are performed by LAMMPS and its output files are used in Ovito environment for visualising and colouring molecules. The MD simulations were performed the use of adaptive intermolecular reactive bond order (AIREBO) potential originated from the second-generation many-body inter-atomic Tersoff-Brenner potential (REBO). The adaptive nature of the AIREBO potential allows an investigation on the welding and mechanical deformation behaviour of hydrocarbon molecules accurately by allowing bond breaking and forming mechanisms in covalent bonds. The reactivity of the AIREBO potential enables for the formation and dissociation of covalent bonds throughout the simulation. In order to avoid non-physical strain hardening of the stress-strain curve Cut-off radius of AIREBO potential is set to be the original value 2 Å. This potential is widely used to be one of the most successful potential functions to describe the intermolecular interactions in hydrocarbon systems containing carbon nanostructures such as graphene and fullerenes.

In this study, MD simulations were performed in the isothermal isobaric (NPT) ensemble for reaching equilibration and periodic boundary conditions (PBC) is implemented in all directions. In order to load covalently bounded graphene-fullerene specimens, compressive displacement are employed via ‘erate’ command of the LAMMPS. According to that dimension of the simulation box at compression direction is changed at a constant engineering strain rate. Before the application of compressive loading, all molecular specimens is exposed to zero pressure and 300 K temperature up to reach equilibrated state. The initial specimens are relaxed for 50 ps at a time step size of 1 fs to ensure the system equilibrium. Energy profiles are monitored during the equilibration process in order to assess thermodynamic stability of graphene-fullerene structure.

After the thermalization of the system, compressive uniaxial displacements are employed with various temperatures and strain rates. All models are tested on room temperature, 300K and we also use 500K and 700K to investigate the temperature dependence. In addition to find out temperature sensitivity of generated models, in this study, it has been initiated to examine understanding of the effects of reasonable strain rate on mechanical behaviour and energy absorption. In this regard, three different strain rates, which are 0.002 1/ps, 0.004 1/ps and 0.006 1/ps, are applied same fullerene-graphene specimens. Moreover, time step is kept at 0.001 ps and the total load duration is set to 1 ps. This time-step obtains a good balance between accuracy and computational cost. Atomic forces, stress and strains are calculated every 1000 steps. The computed time-averaged atomic stresses are used for obtaining the stress-stress curves for each specimen.

6. RESULTS AND DISCUSSIONS

In this research, the compressive behaviour of a novel nanomaterial, namely fullerene-graphene nano–sandwich structures were conducted via LAMMPS. In order to describe elastic mechanical properties and energy absorbing characteristics, comparisons are carried out between fullerene-graphene composite structures with randomly and ordered distributed fullerenes. Furthermore, numerical compression tests are performed on the atomistic models of the nano-sandwiched fullerene-graphene hybrid structures to evaluate strain rate and various temperature impacts on their compressive deformation behaviour.

In order to validate thermodynamic viability of the novel nano-sandwiched foam material, potential energy profiles of four atomistic specimens, which are composed of distinctly structured fullerenes randomly and evenly, are monitored during the thermalization period. For a stable thermodynamic behaviour, it is expected that overall free energy of the specimens must be minimized and must retain the equilibration state in time. According to that, in Figure 6.1, the energy profiles of the specimens in the period of 50 ps obtained by molecular dynamics simulations of thermalization are presented. Based on these results, it is noticed that all configurations reach to equilibrium state in a short time comparing to total simulation time and remained.

Besides that, in order to maintain the temperature of the system the Nose-Hover thermostat is used which provides good conversion of the energy and reduce fluctuation in temperature in the thermalization period. For this study the periodic boundary condition was applied and the pressure was fixed to be 1 bar for all specimens. Before loading, the initial structure is relaxed for 50 ps to ensure that the system is in equilibrium especially because of applying different temperature. According to Figure 6.2, it is apparent that at the end of the first 10 ps all specimens under various temperatures reach to stabilization and 50 ps is quite adequate.

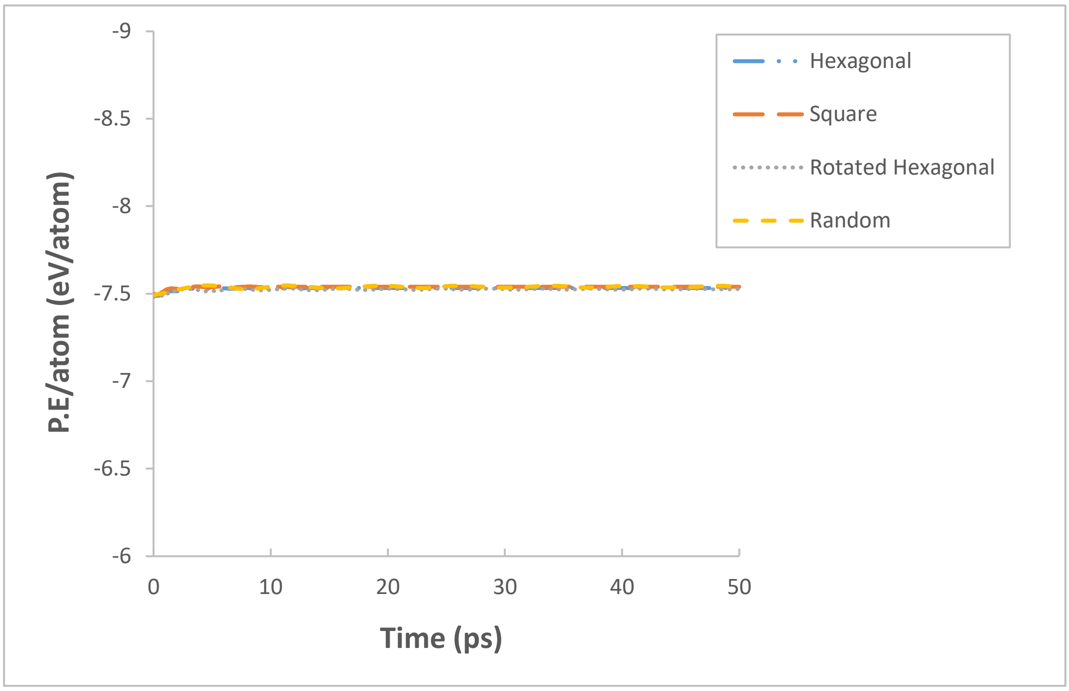

Figure 6.1: Potential energy profile of the nano-sandwiched models with time. The energy is normalized per atom.

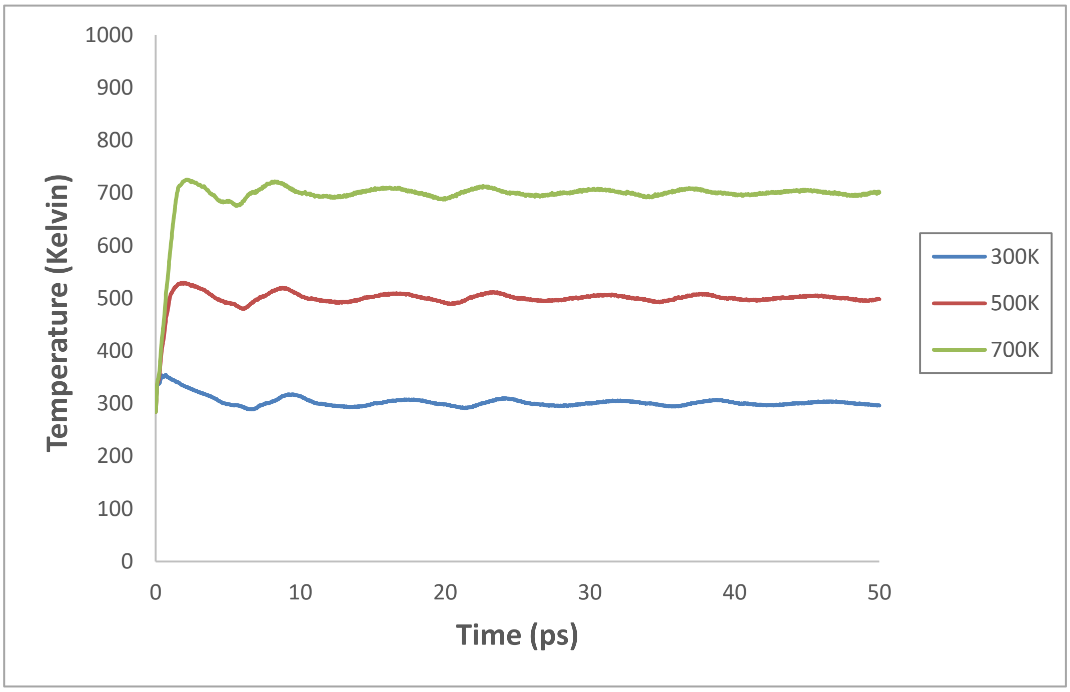

Figure 6.2: Temperature stabilization during the thermalization period for various temperature levels.

6.1 Ordered and Randomly Distributed Fullerenes Between Graphene Layers Models Compressive Behavior Comparison Under Constant Strain Rate and Temperature

The main outcome of the compressive loading experiment is the load versus elongation curve, which is subsequently converted into a stress versus strain curve. Stress-strain curves obtained for the nano-sandwiched models consisting of four different fullerene-graphene hybrid models are presented in Figure 6.3. In the plot, comparison of the nominal stress-strain relationships captured by uniaxial compression tests at the same strain rate is presented.

Instead of a quantitative analysis, at the first sight, the pattern of the stress–strain curves is examined to understand the compressive behaviour of the nano-sandwiched FGs. In this regard, stress-strain curves associated with hexagonal and square fullerene arrangements demonstrate a similar behaviours which are basically defined for nominal stress-strain curve of foamed material, whatever they were made of, obtained by compression testing. Increase of stress appears to be elastic for small compression region up to %10 strain and deformation on the specimens are fully reversible in accordance with stress-strain response of the hexagonal and square fullerene arrangement results.

Besides, the young modulus of the hexagonal and square arrangements express with the initial slope of the stress-strain curve and the compressive stress can be determined by Hook low for linear elastic region. The linear elasticity region in hexagonal and square arrangements is explained by stretching of the cell walls in case of closed cell foams and bending of the cell wall for open-cell foams. After the initial increase of stress there is then a change to a regime of very strong plastic deformation characterized by a small slope of the stress-strain curve. FGs that have a plastic collapse stress, collapse plastically when loaded beyond the linear-elastic regime. Plastic collapse gives a long, approximately horizontal, plateau to the stress strain response. In compression the stress-strain response for polymeric foams will show an extensive plateau at a stress level which doesn’t change much. In compression, the plateau is totally associated with collapse of the cells. This stress level is referenced to as the elastic collapse stress and the slope of the plateau in the stress-strain diagram is called the Plateau modulus in here. The elastic collapse in foams is caused by the elastic buckling of cell walls. Advantage from the long stress plateau is taken in crash protection, since the energy absorption per unit of volume is defined as the area under the stress-strain responses. Like elastic buckling, the failure is localized in a band transverse to the loading direction. This band propagates throughout the foam with increasing strain. For the characterization of foams and the evaluation of their potential applications a determination of their compression behaviour, or, more specifically, their compression strength and the length and slope of the plateau is important.

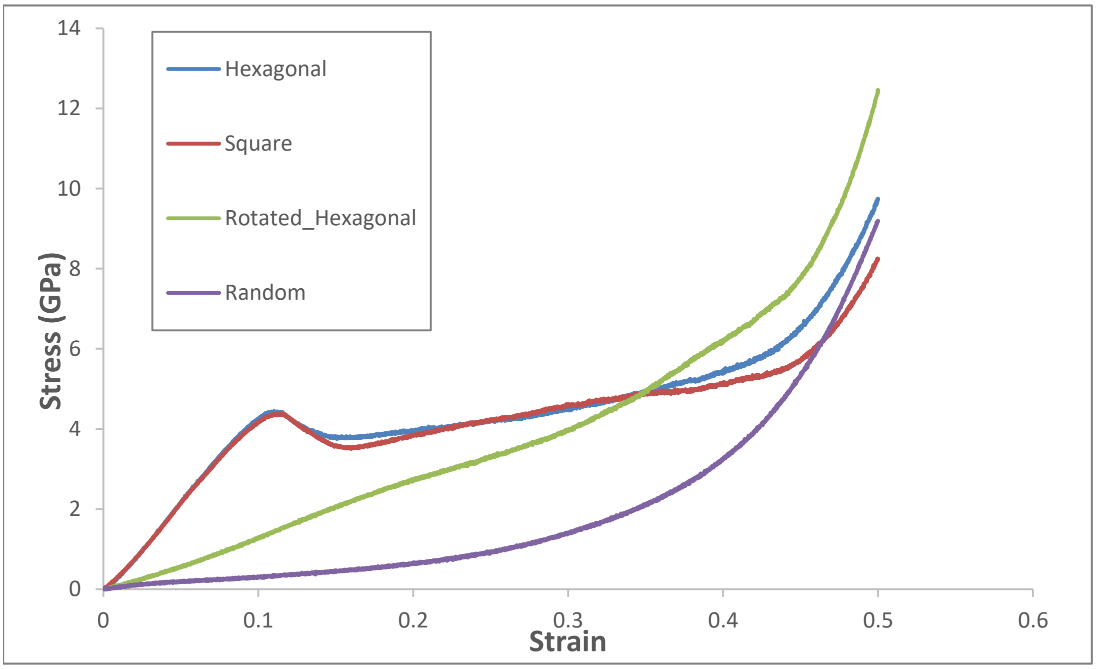

Figure 6.3: Comparison stress-strain curves for the nano-sandwiched structures with different types of fullerene arrangement under 300K room temperature and 0.002 1/ps strain rate.

After an extended plateau regime the stress-strain curve gradually changes into the regime of densification when the cell walls touch each other, accompanied by a steep increase of stress. When the cells have almost completely collapsed opposing cell walls touch and further strain compresses the solid itself, giving the final region of rapidly increasing the relative density of the foam increases the young modulus ,raises the plateau stress and reduces the strain at which densification begins. Snapshots from compressive testing of Fullerene-graphene foam with hexagonal fullerene arrangement is presented Figure 6.4.

Strain-strain graph can also be utilized to compare the compressive response of FG specimens in order to underline the hexagonal and square fullerene arrangement effect of the mechanical behaviour. Slopes, or namely Young modulus, of the initial linear region for two nano-sandwich specimens seem to be approximately same, while the specimens with square fullerene arrangement have slightly less stresses at the end of the buckling and the beginning of the plateau regime. Besides, it can be obviously noticed that the duration of the plateau period and slope of the plateau are almost same. On the other hand, the major differences between the compressive responses of the specimens are observed at the densification and near-densification regions. In these regions, stress level difference of the two specimens increases sharply and hexagonal fullerene arrangement model reaches higher stress levels in a short period.

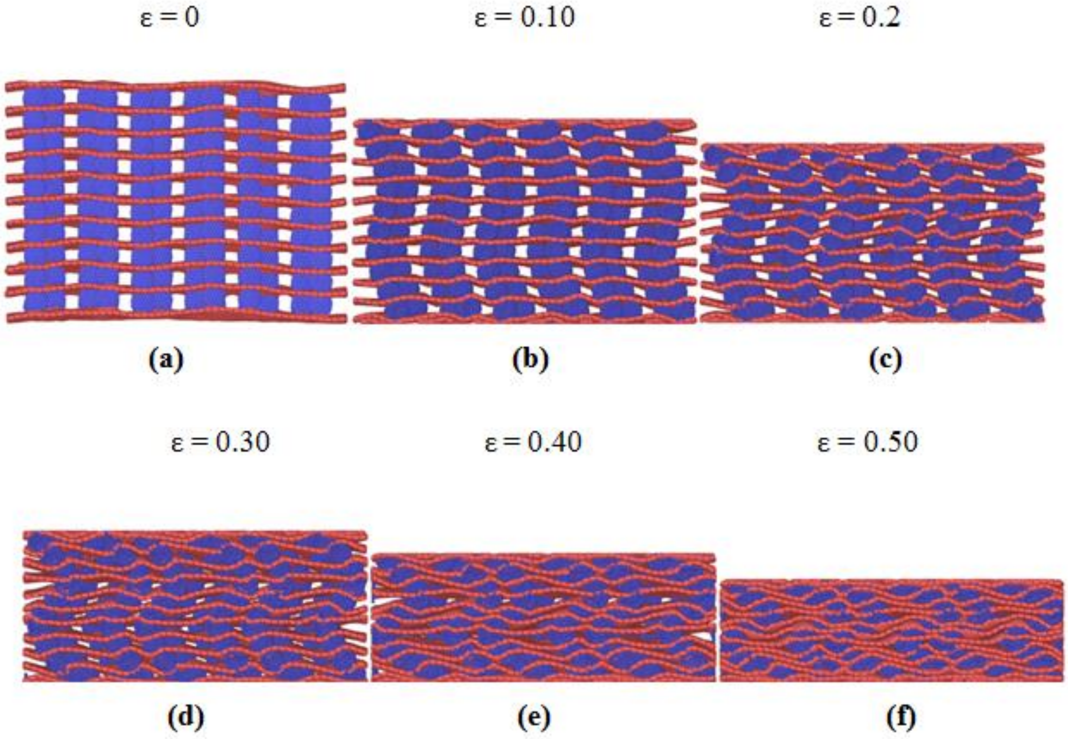

Figure 6.4: Snapshots from compressive testing of Fullerene-graphene foam with hexagonal fullerene arrangement under 300K room temperature and 0.002 1/ps strain rate.

Due to rotated hexagonal arrangement specimens unique spatial fullerene distribution in which fullerenes are located on graphene sheets hexagonally and this structure is rotated 60° in each graphene-fullerene layers respect to graphene sheet centre, rotated hexagonal specimen exhibits totally different compressive stress-strain responses. In this case, slope of the stress-strain curve is approximately constant up to %30 strain rate and the stress increase at which elastic collapse occurs, shows almost linear characteristic. Based on rotated hexagonal structure, fullerenes are not overlapped between two following graphene layers, however, each graphene layer has same fullerene distribution with two graphene layers below and upper. Hence, initial wall bending or stretching of the cell walls occur much faster than randomly fullerene distributed specimen while move much slower than hexagonal/square fullerene distributed models. When the graphene sheets have almost completely collapsed and fullerenes on the different graphene layers touch each other. Further compressive loading constitutes quick buckling period as shown in Figure 6.5 and ends up final region of rapidly increasing stress which may be referred to as densification. It is apparently observed that rotated hexagonal specimen has reached much higher peak stress at %50 strain in comparison with all other test specimens under uniaxial compressive loading and constant strain rate.

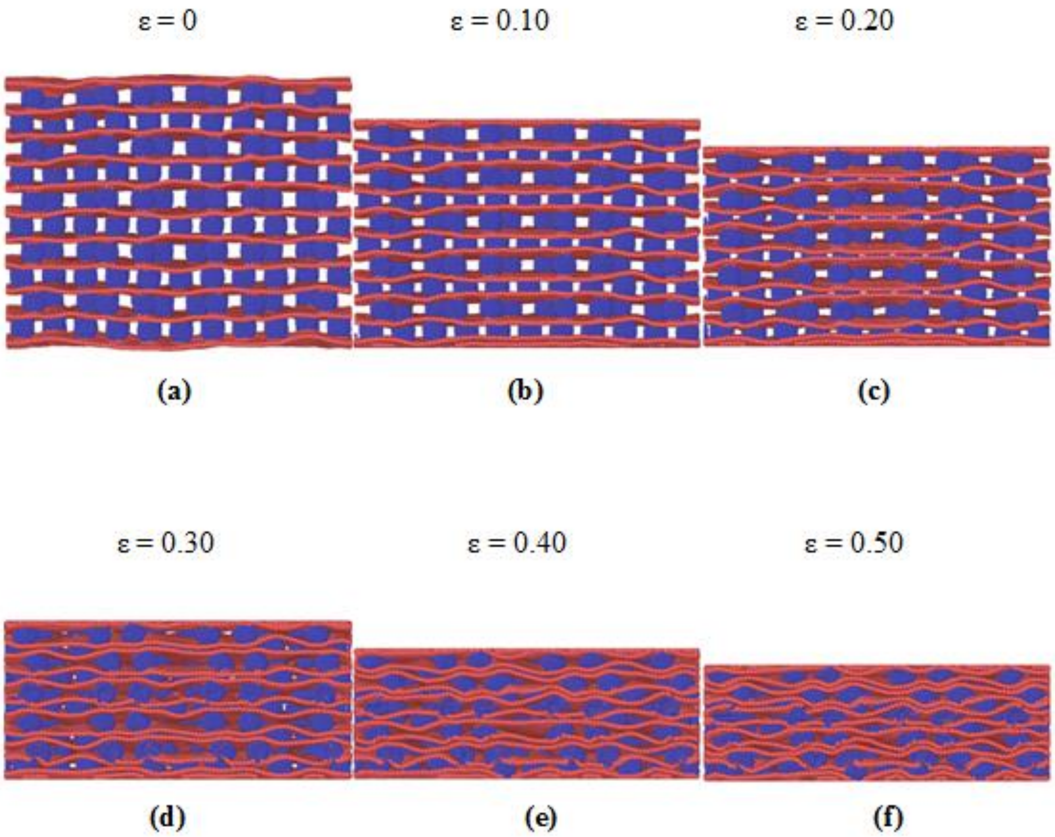

Figure 6.5: Snapshots from compressive testing of Fullerene-graphene foam with rotated-hexagonal fullerene arrangement under 300K room temperature and 0.002 1/ps strain rate.

Considering the compressive stress-strain relationship of hexagonal and square fullerene arrangement specimen structures exhibit similar characteristic with conventional foam materials, just mentioned above, rotated hexagonal and randomly fullerene arrangement specimens introduce absolutely different stress-strain response due to their special fullerene distributions on the graphene layers. As randomly fullerene distributed model is investigated, it may reveal that the initial linear elastic regime does not appear and the plateau regime is not apparently constant under compressive loading. There are non-occupied volumes below each fullerene allowing downwards motion of fullerene junctions without a remarkable resistance due to special arrangement of the fullerenes that is mentioned in the previous section. As a result of that, if the nano-sandwiched structures with fullerene cores are considered as closed-celled foams where the fullerene expose stretching would be expected, fullerene walls are not subjected to considerable stretching in this deformation phase and therefore a distinct linear elastic regime, which is formed in case of hexagonal and square fullerene arrangement specimens , does not appear. Instead of two unique regimes (i.e. linear elastic and plateau), the regime before the densification of the nano-sandwiched structures can be characterized as combination of linear elastic and plateau regimes that may be called as linear-plateau regime. In nano-sandwiched Fullerene-graphene specimen with randomly fullerene arrangement, as the compressive displacement is applied on the top and bottom layers depend on specified strain rate, a compression zone is formed initially and transferred through the rest of the structure in a layer wise manner by decreasing the distance between relaxed graphene sheets, namely relaxed inter-layer distance. Resistance of fullerenes to further compression enables to transfer the compression affect onto the lower layers. As a consequence of this load transfer process, the thickness of the relaxed graphene sheets decreases while the layers sufficiently away from the compression zone remain relaxed and unaffected from the compression. As the number of compressed layers increases, overall compression resistance of the specimen also increases by the inclusion of new fullerenes to bear the compression loading, which results in non-constant plateau region. In contrary to conventional foams, a distinct plateau regime does not exist for the purposed randomly fullerene arrangement nano-foam, just because there is not such a phenomenon of cell collapsing at around constant amplitude loading. Densification is realized by the propagation of the compression zone which decreases the inter graphene distance and induces compressive affect to neighbour layers. As a results of this distinction in the densification process, constant load regime is replaced by a load regime which is continuously increasing. Existence of such a plateau-like regime in the stress-strain curve of randomly fullerene arrangement specimen, as shown Figure 6.3, indicates their energy dissipation property under compressive loading, which may promote their potential usage in energy-absorbing applications similar to conventional foams. Snapshots from compressive testing of Fullerene-graphene foam with randomly fullerene arrangement is presented Figure 6.6.

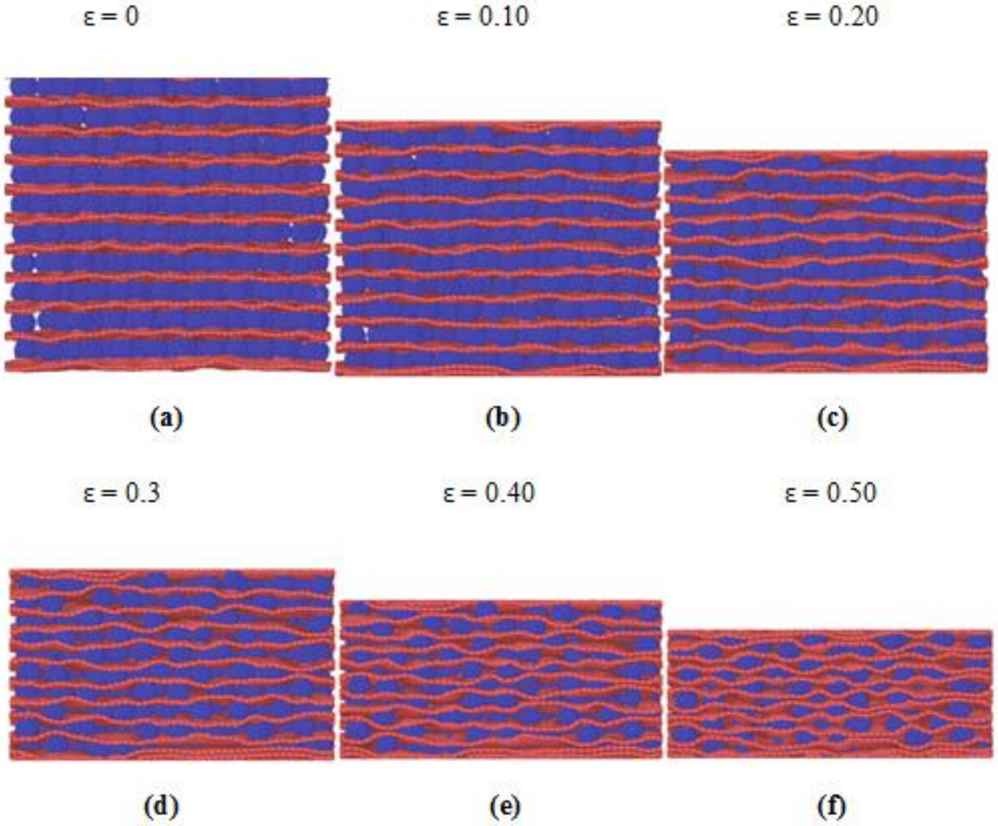

Figure 6.6: Snapshots from compressive testing of Fullerene-graphene foam with randomly fullerene arrangement under 300K room temperature and 0.002 1/ps strain rate.

6.2 Ordered and Randomly Distributed Fullerenes Between Graphene Layers Models Compressive Behavior Comparison Under Constant Strain Rate and Various Temperatures

In addition to comparisons performed between fullerene-graphene composite structures with randomly and evenly distributed fullerenes in terms of elastic mechanical properties and energy absorbing characteristics, we also use 300K, 500K and 700K to investigate the temperature dependence. Effects of temperature on the stress-strain response of the hexagonal fullerene arrangement specimens was seen during the quasi-static loading as seen in Figure 6.7. Concerning this, stress-strain response of the hexagonal arrangement under different temperatures exhibits similar characteristic during the initial linear region and slope of the stress-strain curves are quite equal each other. On the other hand, the plateau stresses are found to be slightly reduced by an average of ~0.2 GPa at 500K and ~0.3 GPa at 700K at the beginning of the plateau regime. Plateau slope of three cases are almost same during the plateau regime while the stress difference decreases at densification period at same strain.

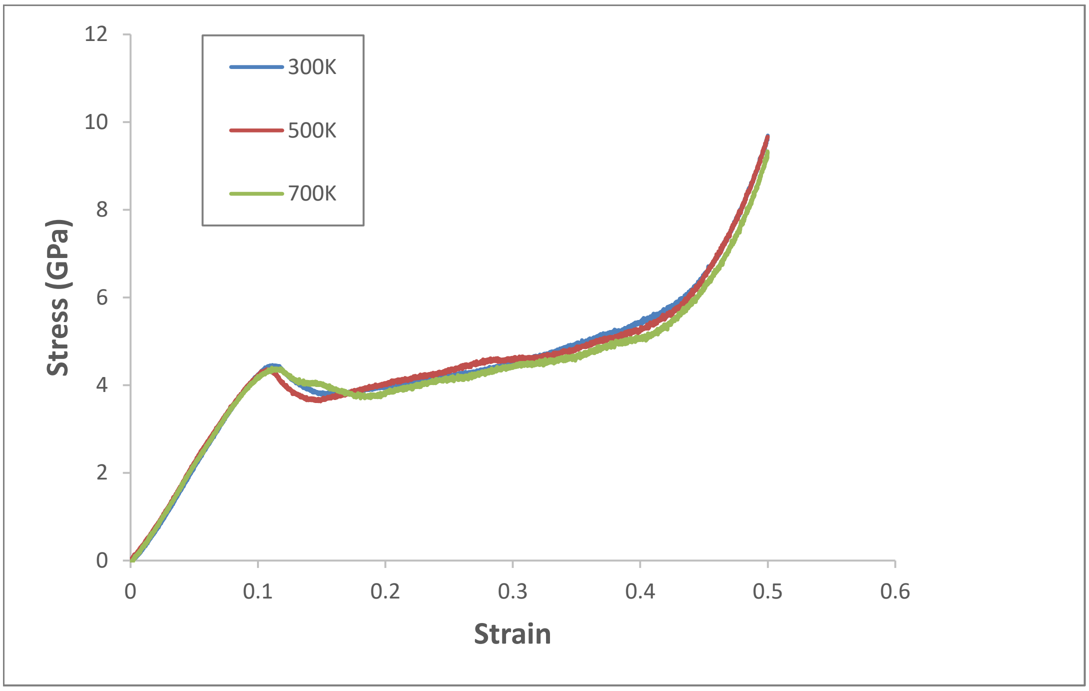

Figure 6.7: Hexagonal fullerene arrangement results under various temperature at 0.002 1/ps strain rate.

When the square fullerene arrangement strain-stress response of square fullerene arrangement, as illustrated Figure 6.8, is investigated, it may noticed that stress-strain response changes exhibit same characteristic with hexagonal fullerene arrangement specimens. Stress-strain responses of the rotated hexagonal and randomly fullerene arrangement models are illustrated in Figure 6.9 and Figure 6.10 respectively. It can be interpreted from corresponding figures that in each model young modulus varies a little with temperature increment. The young moduli trend tend to decrease with an increasing temperature. As a consequence of that, stress level of the rotated-hexagonal and randomly fullerene arrangement models decrease due to temperature increase at the same strain ratio.

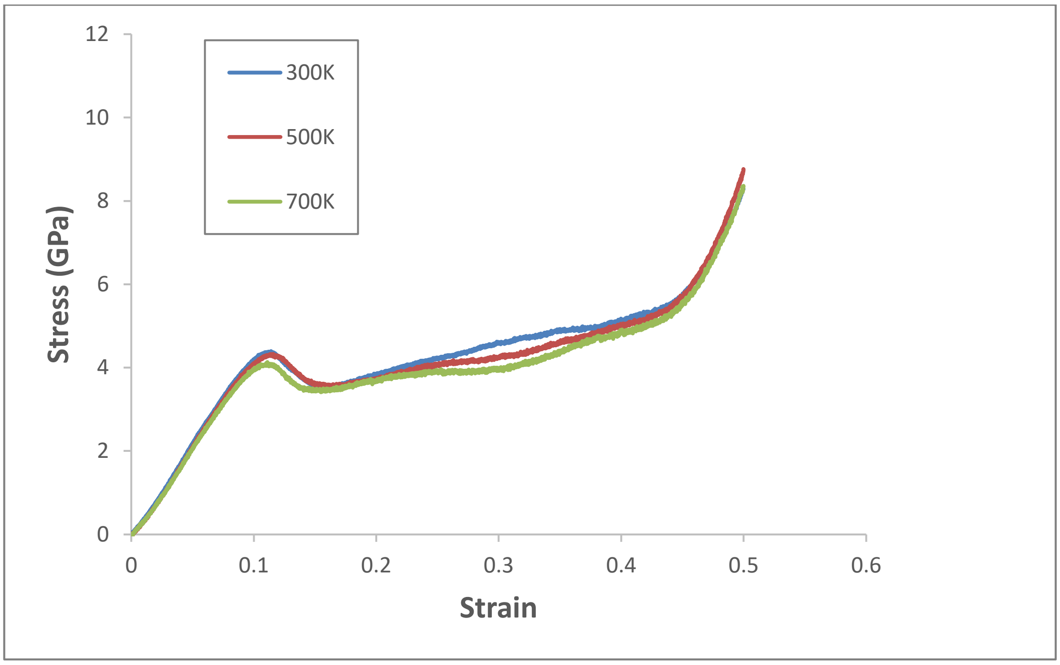

Figure 6.8: Square fullerene arrangement stress-strain curve under various temperatures at 0.002 1/ps strain rate.

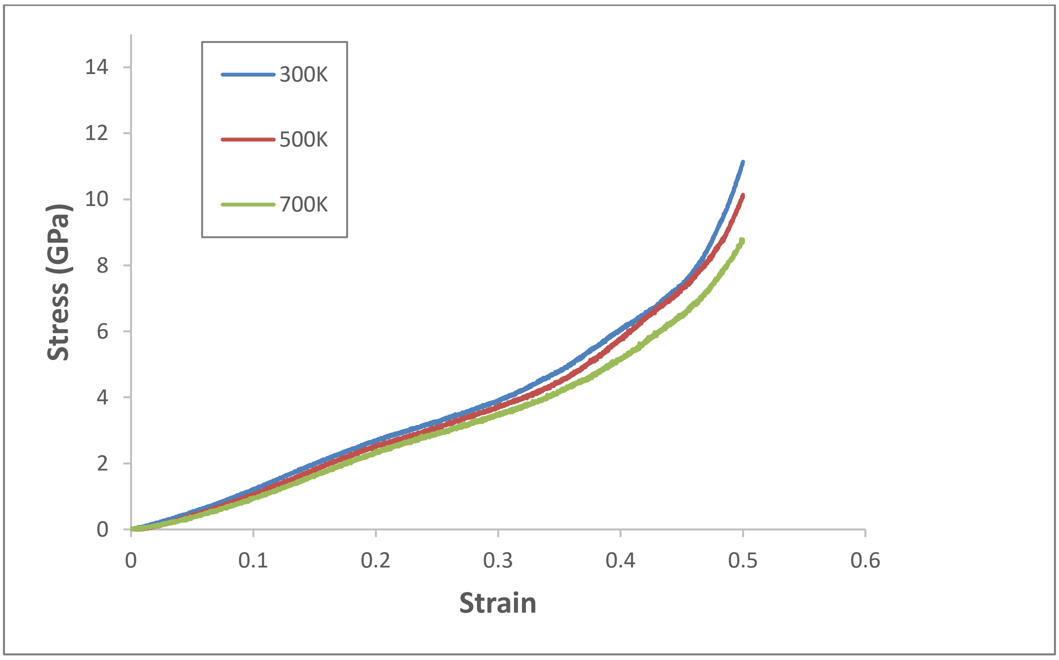

Figure 6.9: Rotated-hexagonal fullerene arrangement results under various temperature at 0.002 1/ps strain rate.

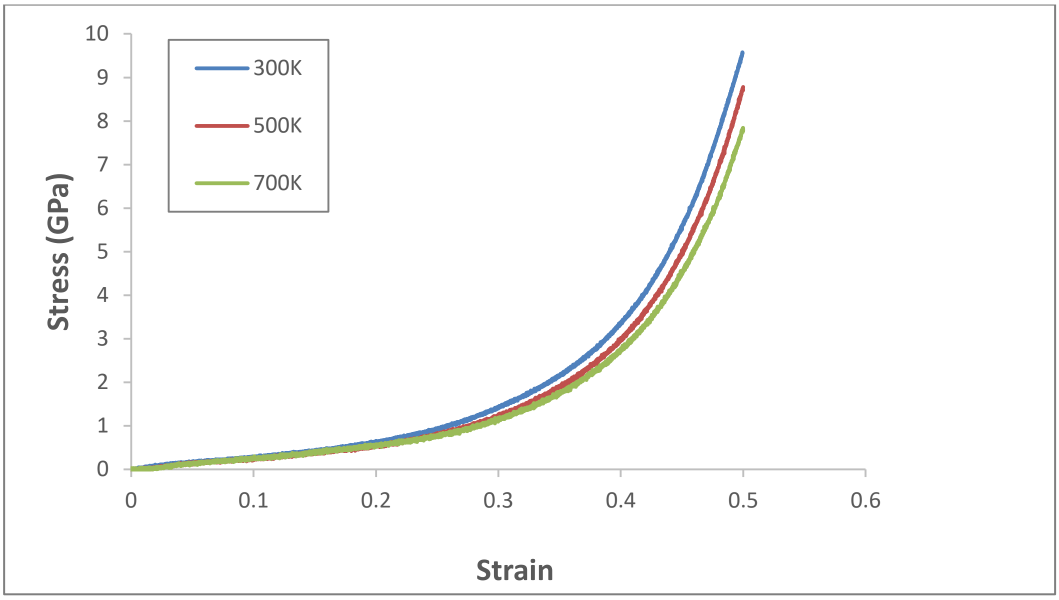

Figure 6.10: Randomly fullerene arrangement results under various temperature at 0.002 1/ps strain rate.

6.3 Ordered and Randomly Distributed Fullerenes Between Graphene Layers Models Compressive Behaviour Comparison Under Various Strain Rate and Constant Temperatures

Another parameter, which is investigated in this study, is strain rate sensitivity. The compressive engineering stress versus engineering strain response of the all Fullerene-graphene specimens were found to be sensitive to be exposed strain rate which are 0.002 1/ps, 0.004 1/ps and 0.006 1/ps. The linear region stresses were found to be parallel up to %10 strain ratio a small average increase due to strain rate increase for hexagonal and square fullerene arrangement specimens. The yield strength displayed greater dependence on strain rates for hexagonal and square fullerene distributed specimens as illustrated Figure 6.11 and Figure 6.12.The plateau strength of the plateau strength of the hexagonal fullerene arrangement specimens at 0.002 1/ps, shown in Figure 6.11, increased from ~4.6 GPa to ~4.9 GPa at 0.004 1/ps to ~5.1 GPa at a strain rate of 0.006 1/ps. In addition to plateau stress changes, slope of the plateau is decreased and shorter plateau regime period is occurred under higher strain rates. For instance, according to Figure 6.13, densification regime begins at %43 strain ratio at 0.002 1/ps, %37 strain ratio at 0.004 1/ps and %31 strain ratio at 0.006 1/ps for rotated-hexagonal fullerene arrangement specimens. As a consequence of the linear and plateau regime stress level and characteristic, for the all models tested in this study, the absorbed energy was found to slightly decrease with higher strain rate until the evaluation point which is near the transition foam wall collapse and material densification regime.

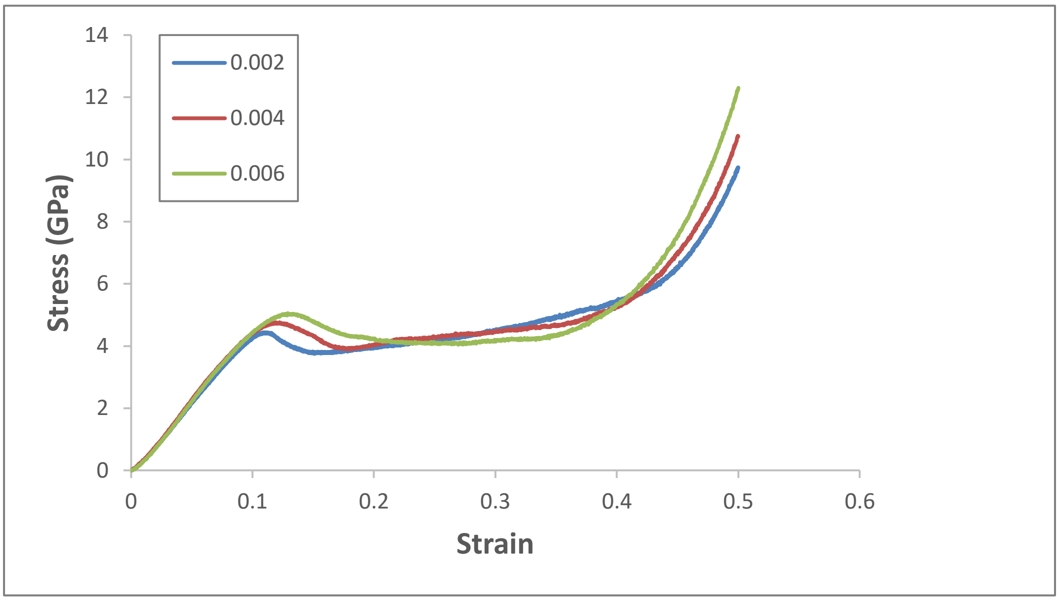

Figure 6.11: Hexagonal fullerene arrangement stress-strain curve under various strain rate 300 K.

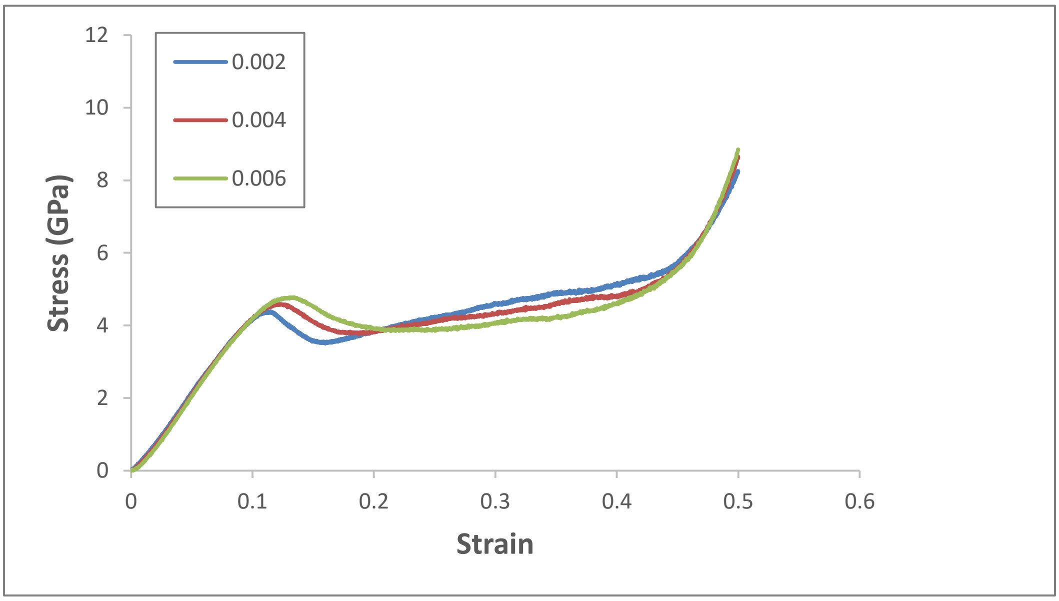

Figure 6.12: Square fullerene arrangement stress-strain curve under various strain rate 300 K.

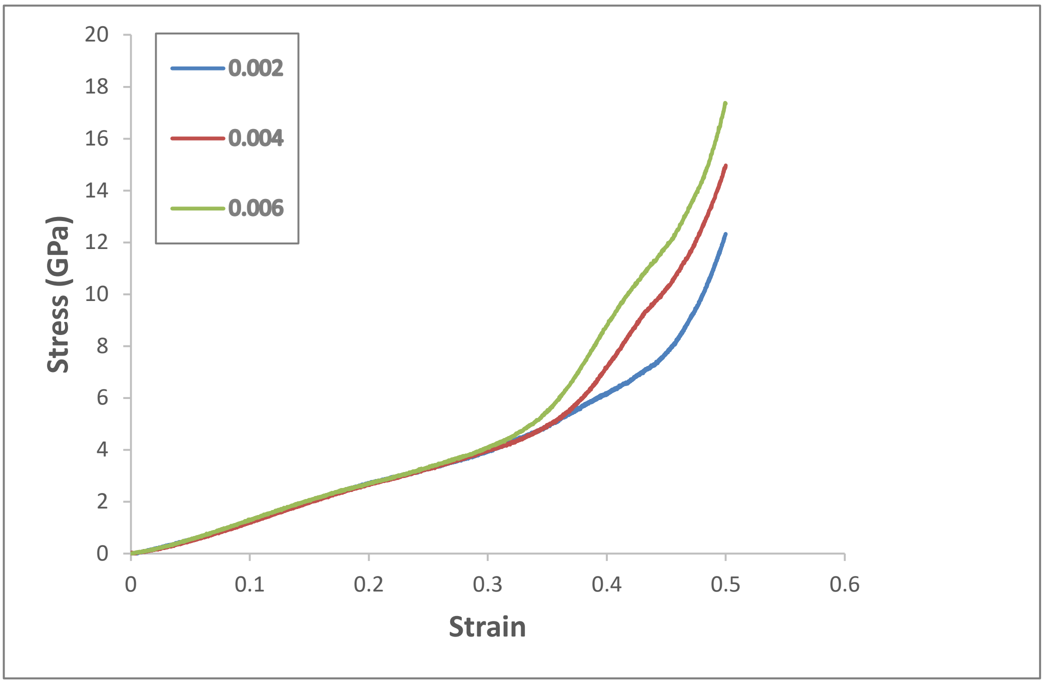

Figure 6.13: Rotated-Hexagonal fullerene arrangement stress-strain curve under various strain rate at 300 K.

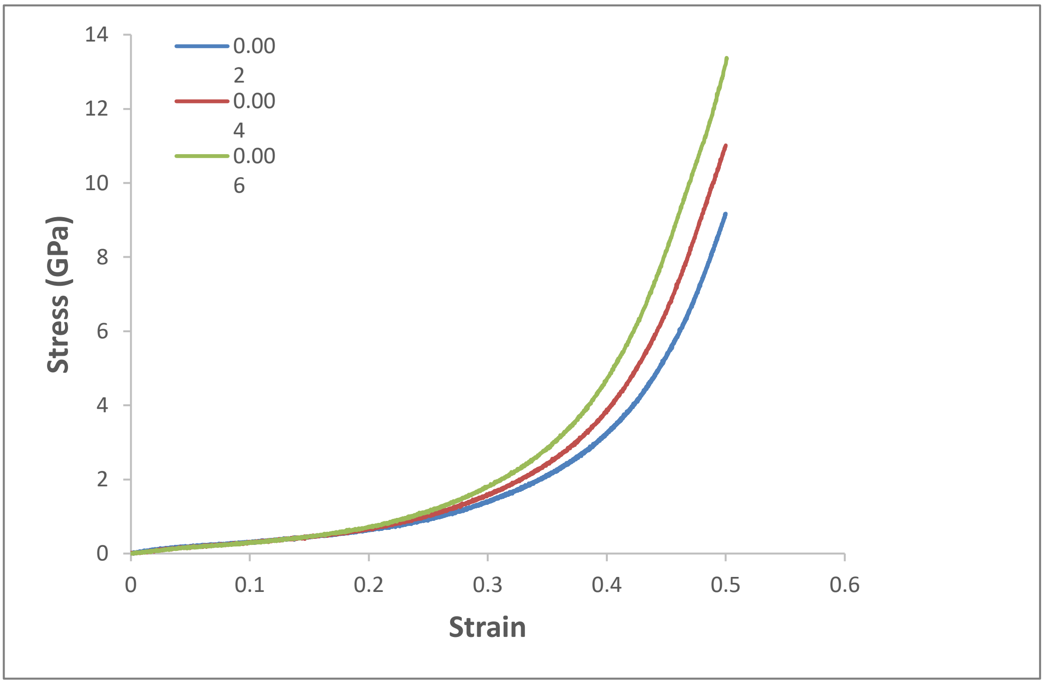

Figure 6.14: Randomly fullerene arrangement stress-strain curve under various strain rate at 300 K.

7. CONCLUSION AND RECOMMENDATIONS

The mechanical behaviour of novel fullerene-graphene nano-foam materials were studied through the MD simulations under uniaxial compressive loading. In the MD simulations, the four nanostructures were assumed to be different spatial fullerene arrangement between graphene layers and results were compared. It was found that spatial distribution of fullerenes has remarkable influence on both compressive stress level and stress-strain characteristic of the novel fullerene–graphene foams. Mechanical response of the hexagonal and square fullerene arrangement models are in good agreement with both each other and conventional foam materials while rotated hexagonal and randomly fullerene distributed models are exhibited totally unique mechanical behaviours due to their special structures .In addition to investigation of spatial fullerene distribution effects on mechanical properties of the fullerene-graphene specimens, temperature and strain rate sensitivity of nano foams are studied in this thesis. As a consequence of certain MD simulation results, applied temperatures have no major impact on stress-strain curve tendency; however, young modulus of the materials tend to decrease with higher employed temperature level. In parallel that mechanical tests of fullerene-graphene foams under uniaxial compression show that the form of the stress-strain diagram does not depend on the applied strain rates. However, higher strain rates in general lead to higher stresses under compression at the beginning of the plateau regime and densification phase.

There are several topics which can recommend as further tasks in order to understand mechanic behaviour of novel fullerene-graphene nano-foam material. First of all, in order to capture thermal sensitivity much more accurately, extend the temperature range, for instance; temperature may vary between 0 K to 1200 K according to certain papers. Additionally, Micro-inertial effects are being crucial at a critical strain rate in respect to some other researches. Hence, it may be recommended that defining this threshold may help to understand strain rate sensitivity more apparently. As a final recommendation, analysis may be repeated up to different strain level in order to identify reversible elastic deformation limits of fullerene-graphene materials. Thus, relaxation phase should be added to LAMMPS script just after deformation phase.

REFERENCES

[1] **Mohammadi, M., Ghayour, M., & Farajpour, A.** (2013). Free transverse vibration analysis of circular and annular graphene sheets with various boundary conditions using the nonlocal continuum plate model. *Composites Part B: Engineering*, *45*(1), 32–42. http://doi.org/10.1016/j.compositesb.2012.09.011

[2] **Spyrou, K., Kang, L., Diamanti, E. K., Gengler, R. Y., Gournis, D., Prato, M., & Rudolf, P.** (2013). A novel route towards high quality fullerene-pillared graphene. *Carbon*, *61*, 313–320. http://doi.org/10.1016/j.carbon.2013.05.010

[3] **Montazeri, A., Ebrahimi, S., & Rafii-Tabar, H.** (2015). A molecular dynamics investigation of buckling behaviour of hydrogenated graphene. *Molecular Simulation*, *41*(14), 1212–1218. http://doi.org/10.1080/08927022.2014.968849

[4] **Ansari, R., Sadeghi, F., & Ajori, S.** (2013). Continuum and molecular dynamics study of C_{60} fullerene-carbon nanotube oscillators. *Mechanics Research Communications*, *47*, 18–23. http://doi.org/10.1016/j.mechrescom.2012.11.002

[5] **Kal, R. Sharma**, (2014).*Graphene Nanomaterials, New York: Momentum Press.*

[6] **Zhong, Z**.(2012).*Carbon Nanotubes as Nanodelivery Systems: An Insight Through Molecular Dynamics Simulations.*

[7] **Karličić, D., Cajić, M., Kozić, P., & Pavlović, I.** (2015). Temperature effects on the vibration and stability behavior of multi-layered graphene sheets embedded in an elastic medium. *Composite Structures*, *131*, 672–681. http://doi.org/10.1016/j.compstruct.2015.05.058

[8] **Cosden, I. A., & Lukes, J. R.** (2013). A hybrid atomistic-continuum model for fluid flow using LAMMPS and OpenFOAM. *Computer Physics Communications*, *184*(8), 1958–1965. http://doi.org/10.1016/j.cpc.2013.03.009.

[9] **Plimpton, S.** (1995). Fast Parallel Algorithms for Short-Range Molecular Dynamics. *Journal of Computational Physics*. http://doi.org/10.1006/jcph.1995.1039.

[10] **Hardev, S. Virk**. *Solid State Phenomena: Nano Materials Basic Concepts and Applications*, Trans Tech Publications, 2015.

[11**] Vajtai, R.,** (2013). *Springer Handbook of Nanomaterials,* Springer, Berlin, Heidelberg, 2013.

[12] **Yury, Gogotsi** (1982). *Design Recommendations For Cyclic Loaded Welded Structures*. Welding in the World, 20(7/8), pp. 153-165

[13] **Kırca, Mesut.** *Mechanics of nanomaterials consisted of random networks,* Istanbul Technical University, Dissertations, 2013.

[14] **Ramesh, K. T.,** (2010). *Nanomaterials: mechanics and mechanism*. New York, Springer, 2010.

[15] **Harry, M., Edward Heintz A., and Francisco, R. R.,** (1997). *Introduction to carbon technologies*, University of Alicante, 1997.

[16] **Harry, M., Edward Heintz A., and Francisco, R. R.,** (2000). *Science of carbon materials*. University of Alicante, 2000.

[17] **Vijay, K. Varadan,** (2010).*Nanoscience and Nanotechnology in Engineering,* University of Arkansas, USA.

[18] **Andreas, H., and Michael, B.,** (2005). *Fullerenes: chemistry and reactions*. Weinheim, Great Britain.

[19] **Eiji, O., (2002).** *Perspectives of Fullerene Nanotechnology,* Nano carbon Research Institute, Chiba, Japan

[20] **Charles, M., Lieber,** (2006). *Preparation of fullerene and fullerene-based materials*, Harvard University.

[21] **Anke, Krueger**, (2010).*Carbon Materials and Nanotechnology, WILEY-VCH Verlag GmbH & Co. KGaA, 2010.*

[22] **Roberto, Munoz., Garcia, Hernandez., & Cristina, Gomez.** *Handbook of Carbon Nano Materials, Chapter 4, CVD of Carbon Nano Materials,* Singapore: World Scientific Publishing Co. Pte Ltd., 2016.

[23] **Swapan, K. P., Toshiaki, E., and Rao, C. N. R.,** (2011). *Graphene and Its Fascinating Attributes,* World Scientific.

[24] **Nitin, C., and Wonbong, C.** *Handbook of Carbon Nano Materials, Chapter 1, Graphene Synthesis and Applications*. Department of Materials Science and Engineering, University of North Texas, USA.

[25] **Jarosaw, M., (2001).** *Molecular Dynamic,*Cornell University, Encyclopedia of Life Sciences.

[26] **Rapaport, D. C.** *The Art of Molecular Dynamics Simulatıon (Second Edition),* Cambridge University Press, 2004.

[27] **Url-1 <**http://lammps.sandia.gov>, date retrieved 10.05.2016.

APPENDICES

APPENDIX A: Lammps Script

APPENDIX A

```
# 3D Graphene-Fullerene Lammps Simulation

# ----------------------------------------Initialization Phase-------------------------------------

dimension  3
boundary   p p p
atom_style atomic
units  metal
neighbor 2.0 bin
neigh_modify every 1 check no

#----------------------------------------Atom Definition Phase---------------------------------

read_data graphene_welding.dat

#--------------------------------------Force Field Definition Phase----------------------------

pair_style airebo 2.5 1 0
pair_coeff * * CH.airebo C C
mass   1  12.0
mass   2  12.0
include include.dat

#----------------------------------------Minimization Phase-------------------------------------

dump 1000 all atom 500 dump_minimize.lammpstrj
minimize 1e-6 1e-6 1000000 1000000
undump 1000

#----------------------------------------Equilibration Phase-------------------------------------

thermo_style custom step temp pe etotal press vol c_mytemp
```

```
variable stemperature equal 700 # temperature in kelvin
variable epercentage equal 0.75 # the percentage the body is compressed 0.5
variable myseed equal 887723 # the value seed for the velocity 12345
variable atomrate equal 10000 # the rate in timestep that atoms are dump as CFG 2500
variable time_step equal 0.001 # time step in pico seconds 0.001
variable time_eq equal 50000 # time steps for the equlibration part
variable tdamp equal "v_time_step*100" # DO NOT CHANGE
variable pdamp equal "v_time_step*1000" # DO NOT CHANGE
variable R equal 0.002 # ERATE here 0.005 1/ps every picosecond 0.005
variable time_run equal "(v_epercentage/v_R)/v_time_step"
timestep ${time_step} # DO NOT CHANGE

compute myKE all ke/atom
compute myPE all pe/atom

compute str all stress/atom NULL
compute 55 all reduce sum c_str[3]

reset_timestep 0
dump 1000 all atom 1000 dump_equil.lammpstrj

fix equilibration all npt temp ${stemperature} ${stemperature} ${tdamp} iso 0 0 ${pdamp} drag 0.200

variable eq1 equal "step"
variable eq2 equal "-pxx/10000"
variable eq3 equal "-pyy/10000"
variable eq4 equal "-pzz/10000"
variable eq5 equal "lx"
variable eq6 equal "ly"
variable eq7 equal "lz"
variable eq8 equal "temp"
variable eq9 equal "etotal"
variable strzz equal c_55
variable strzzv equal c_55/vol

fix output1 all print 20 "${eq1} ${eq2} ${eq3} ${eq4} ${eq5} ${eq6} ${eq7} ${eq8} ${eq9} ${strzz} ${strzzv}" file run.${stemperature}K.out screen no

thermo_style custom step pxx pyy pzz lx ly lz temp etotal
thermo 1000

run ${time_eq}

change_box all z final -23.0 142.0 boundary p p p

variable tmp equal "lz"
variable L0 equal ${tmp}
print "Initial Length, L0: ${L0}"

unfix equilibration
unfix output1
undump 1000

change_box all z final -23.0 142.0 boundary p p p

#---------------------------------------Deformation Phase-------------------------------------

reset_timestep 0
dump 1000 all atom 5000 dump_comp.lammpstrj
fix 1 all nve
fix 2 all langevin ${stemperature} ${stemperature} ${tdamp} 343434
fix 3 all deform 1 z erate -${R} units box remap x

variable strain equal "(lz - v_L0)/v_L0"
variable shear equal "0.5*(pxx/10000 - 0.5*(pyy/10000 + pzz/10000))"
variable tstep equal "step"
variable mypxx equal "-pxx/10000"
variable mypyy equal "-pyy/10000"
variable mypzz equal "-pzz/10000"
variable mylx equal "lx"
variable myly equal "ly"
variable mylz equal "lz"
variable mytemp equal "temp"
variable myvol equal "vol"

variable mystrzz equal c_55
variable mystrzzv equal c_55/vol
fix def1 all print 50 "${strain} ${mypxx} ${mypyy} ${mypzz} ${shear} ${mylx}
${myly} ${mylz} ${mytemp} ${mystrzz} ${mystrzzv}" file
stress.${stemperature}K.${epercentage}e.out screen no

variable thermostep equal "v_time_run/10"
thermo ${thermostep}
thermo_style custom "v_strain" pxx pyy pzz lx ly lz temp etotal pe ke
run ${time_run}

unfix def1
unfix 1
unfix 2
unfix 3
undump 1000
```

CURRICULUM VITAE

Name Surname **:** Uğur Şimşek

Place and Date of Birth **:** İstanbul – 17.08.1988

E-Mail **:** omerugursimsek@gmail.com

EDUCATION :

- **B.Sc.** **:** 2012, Yildiz Thecnical University, Mechanical Engineering Department

PROFESSIONAL EXPERIENCE AND REWARDS:

- 2016 TEI, İstanbul, Stress Engineer
- 2014-2016 TEI/General Electric Aviation-TTC, Gebze, Kocaeli, Stress Engineer
- 2012-2014 Arçelik/BEKO Inc., Cayirova Washing Machine Plant, Design Engineer